



universität
wien

DIPLOMARBEIT

Molecular pharmacology of amantadine and related drugs in cells heterologously expressing human transporters and receptors

angestrebter akademischer Grad

Magister der Naturwissenschaften (Mag. rer.nat.)

Verfasser:	Christian Sommerauer
Matrikel-Nummer:	0040149
Studienrichtung /Studienzweig (lt. Studienblatt):	Diplomstudium Molekulare Biologie
Betreuerin / Betreuer:	Ao.Prof.Dr. Christian Pifl
Wien, am	27. Jänner 2010

Table of contents

I	Summary	3
II	Zusammenfassung	4
1.	Introduction	6
1.1.	Amantadine	6
1.1.1	Chemistry of amantadine	6
1.1.2.	Amantadine as anti-Parkinson adjuvant	7
1.1.3.	dyskinesia in PD	10
1.1.4.	N-methyl- D-aspartate (NMDA) receptors and glutamate in DID	11
1.1.4.1.	The NMDA receptor	11
1.1.4.2.	Glutamate receptor mediated mechanisms in DID	11
1.2.	Implications of the noradrenergic system in PD	13
1.2.1.	Noradrenergic α_2 autoreceptors	14
1.2.1.1.	α_2-adrenoceptor blockers in PD	14
1.3.	Effects of amantadine on DA and NE neurotransmission	15
1.4.	The noradrenaline transporter	17
1.4.1.	NAT structure and function	18
1.4.2.	Tissue expression	20
1.4.3.	Regulation of NAT function	21
1.4.4.	NAT inhibitors	21
1.5.	The dopamine transporter	22
1.5.1.	Function and mechanism of dopamine transport	22
1.5.2.	Protein structure	23
1.5.3.	Uptake blockers	24
1.5.4.	Amphetamine like substances	25
1.6.	Patch-clamp	26
2.	Materials and methods	28
2.1.	Cell culture	28
2.1.1	Cells expressing the DAT or NAT in an inducible manner	28
2.1.1.1.	Transfection using calcium phosphate	30
2.1.2.	Cell lines expressing the human NR1/2A NMDA receptor	31
2.1.2.1.	Subcloning of the NR1 subunit	31
2.1.2.2.	Transient transfection of NR1 and NR2A subunits	37
2.1.2.3.	Stable transfection of NR1 and NR2A subunits	38

2.2.	Patch-clamp experiments	38
2.2.1.	Pipette Puller	39
2.2.2.	Drug application device	40
2.2.3.	Voltage clamp mode	41
2.3.	Uptake-experiments	41
2.4.	Superfusion	42
2.5.	Radioligand binding on NMDA receptor expressing cells	42
2.6.	Cell viability assay	43
3.	Results	46
3.1.	Uptake experiments on NAT or DAT expressing cells	46
3.2.	Release experiments on NAT expressing cells	47
3.3.	Patch-clamp experiments	49
3.3.1.	Patch-clamp experiments on NAT expressing cells	49
3.3.2.	Patch-clamp experiments on DAT expressing cells	53
3.4.	Characterization of cells expressing the human NR1/2A receptor	56
3.4.1.	Radioligand binding after transient transfection	56
3.4.2.	Cytotoxicity after stable transfection	56
3.4.3.	Radioligand binding after stable transfection	58
3.5.	Toxicity assays on NAT or NR1/2A-receptor expressing cells	59
3.5.1.	MPP⁺-induced cytotoxicity in NAT expressing cells	59
3.5.2.	NR1/2A-receptor induced cytotoxicity	62
4.	Discussion	65
5.	References	68
	Curriculum Vitae	74

I Summary

Since the 70s the tricyclic amine amantadine is used as anti Parkinson adjuvans as it could substantially reduce parkinsonian symptoms. Parkinson's disease is characterized by a loss of dopaminergic fibers of the substantia nigra pars compacta but also the noradrenaline rich fibers of the locus coeruleus are affected by neuronal cell damage. Drugs which are restoring dopamine levels in the early stage and noradrenaline levels in later stages are clinically useful. In the 70s it was revealed that amantadine is able to increase central dopamine and noradrenaline levels due to enhanced release or uptake blockade of the dopamine and noradrenaline transporter (DAT and NAT).

In the following work we wanted to assess its role as a possible releaser like amphetamine or uptake blocker on the human DAT or NAT by means of uptake experiments, superfusion experiments and patch clamp, as this was not clarified in the previous studies. The second part of my work was dedicated to the design of n-methyl-d-aspartate (NMDA) receptor (NR1/2A) expressing HEK 293 cells whose NMDA receptor is autotoxic. In several studies amantadine also showed NMDA receptor blocking properties. The potency of amantadine to suppress NMDA receptor mediated autotoxicity was compared with other test drugs like ketamine in cell viability assays. The ability of amantadine to block the entry of the NAT toxin 1-methyl-4-phenylpyridinium (MPP⁺) was also examined.

Uptake experiments showed that amantadine is 15 times more potent in inhibiting the NAT than the DAT. In superfusion experiments amantadine clearly demonstrated a releasing action with a maximum effect less half than that of amphetamine. Patch clamp also revealed that amantadine was a releasing drug at the NAT. On dopamine transporter expressing cells amantadine produced no significant inward currents suggesting a lower affinity at the DAT which is in agreement with the uptake data. In the cell viability assay ketamine blocked cytotoxicity in the μmol range restoring cell viability to more than 90% of that of cells without NMDA receptor induction. Contrary to this, amantadine was only partly protective at 300 μM . In NAT expressing cells the tricyclic antidepressant desipramine had the highest potency in blocking MPP⁺ induced toxicity. Amantadine was less potent than desipramine but 100 μM had a significant effect and 300 μM a strong protective effect restoring cell viability to 80% of vehicle treated cells.

II Zusammenfassung

Seit den 70er Jahren wird das tricyklische Amin Amantadine als Hilfsmittel bei der Parkinson Erkrankung verwendet da es wesentlich dazu beiträgt Parkinson Symptome zu reduzieren. Die Parkinson Erkrankung ist gekennzeichnet durch einen Verlust von dopaminergen Nervenfasern der Substantia nigra pars compacta aber auch Noradrenalin-hältigen Fasern des locus coeruleus die auch von Nervenzellschädigung betroffen sind. Substanzen die den Dopaminspiegel wiederherstellen in der Anfangsphase der Krankheit sowie den Noradrenalin Spiegel in späteren Stadien sind klinisch relevant. In den 70er Jahren konnte gezeigt werden, dass Amantadin fähig ist den Dopamin und Noradrenalin Spiegel anzuheben durch Blockade des Noradrenalin und Dopamintransporters (NAT und DAT) oder durch vermehrte Freisetzung dieser Katecholamine.

In der nachfolgenden Arbeit wollten wir herausfinden, ob Amantadin wie Amphetamin freisetzende Eigenschaften besitzt oder wie ein Wiederaufnahmehemmer am DAT und NAT wirkt. Die Umsetzung erfolgte mittels Uptakeexperimenten, Superfusions- experimenten und Patch clamp, da der genaue Mechanismus in den bisherigen Studien nicht untersucht wurde. Der zweite Teil der Arbeit bestand in der Herstellung von N-methyl-d-Aspartat (NMDA) Rezeptor (NR12A) exprimierenden HEK 293 Zellen deren neuer Rezeptor autotoxisch ist. In einigen Studien konnte gezeigt werden, dass Amantadin als NMDA Rezeptorblocker wirkt. Die Potenz von Amantadin, NMDA Rezeptor vermittelnde Autotoxizität zu unterdrücken wurde in Vitalitätsversuchen an diesen Zellen untersucht. Die Fähigkeit von Amantadin, das NAT Toxin 1-methyl-4-phenylpyridinium (MPP^+) zu blockieren wurde ebenfalls untersucht.

Die Uptake Experimente zeigten, dass Amantadin 15 mal potenter war bei der Hemmung des NAT als des DAT. Bei den Superfusionsexperimenten konnte deutlich bewiesen werden, dass Amantadin einen Freisetzungseffekt besitzt mit einem Maximalwert der weniger als halb so groß ist wie der von Amphetamin. Mit Patch clamp konnte auch gezeigt werden, dass Amantadin ein freisetzendes Substrat am NAT ist. Bei den DAT exprimierenden Zellen produzierte Amantadin keine signifikanten Einwärtsströme was mit einer niedrigeren Affinität am Dopamintransporter zu erklären ist, übereinstimmend mit den Uptake Messergebnissen. Im Vitalitätsversuch konnte Ketamin die Cytotoxizität im $\mu\text{molaren}$ Bereich zu mehr als 90% unterbinden im Vergleich zu Zellen ohne NMDA Rezeptor Bildung. Im Gegensatz dazu war Amantadin bei 300 μM nur teilweise protektiv.

In NAT exprimierenden Zellen hatte das trizyklische Antidepressivum Desipramin die höchste Potenz in der Blockierung der MPP⁺ induzierten Toxizität. Amantadin war niedrigerpotenter als Desipramin, obgleich 100 µM einen signifikanten Effekt verursachten und 300µM einen starken protektiven Effekt zeigten der 80% der Zellen verglichen mit Vehikel behandelten Zellen wiederherstellte.

1 Introduction

1.1 Amantadine

1.1.1 Chemistry of amantadine

The tricyclic amine amantadine is a derivative of adamantane, which itself is a cycloalkane. The molecule consists of adamantane backbone that is substituted at one of the four methylene positions with an amino group. Its known formally as 1-aminoadamantane (Fig. 1).

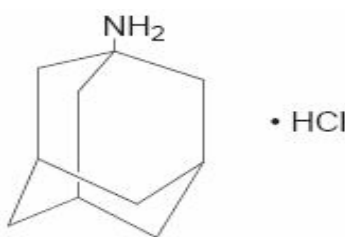


Fig. 1: structural formula of amantadine

Amantadine is well absorbed and has a complete bioavailability. In men, the maximum plasma levels are reached within 1-12 h after oral administration. The mean half life is 10-14 hours, in renal impairment up to 7-10 days. There is a negligible metabolism, thus elimination of amantadine is predominantly renal as unchanged compound (90%, Aoki and Sitar 1985). The drug is highly lipophilic, a passage through the blood-brain barrier depends on the degree of saturation. Toxicological studies indicate a main effect in the central nervous system (Vernier, et al. 1969). Since the 1960s it has been widely used for the prophylaxis and treatment of influenza A. Amantadine acts as an inhibitor of the ionchannel M2, which is one of three important viral integrated membrane proteins. The M2 channel protein is an essential component of the viral envelope because of its ability to form a highly selective, pH-regulated, proton-conducting channel, which is necessary for viral uncoating. In the presence of amantadine, viral uncoating is incomplete, and the ribonucleoprotein core fails to promote infection (Basler 2007).

1.1.2 Amantadine as anti-parkinson adjuvant

Furthermore, observations in the 70s showed, that amantadine is beneficial for the treatment of Parkinson disease (PD), as it could substantially reduce parkinsonian symptoms (Boman and Porras 1970; Grelak, et al. 1970). Parkinson is a degenerative disease of the brain which is characterized by a progressive loss of dopaminergic fibers in the substantia nigra pars compacta innervating the caudatus nucleus and the putamen which together are called striatum, being a part of the extrapyramidal motor system. Moreover, other systems like the noradrenaline (NA) containing locus coeruleus (LC) neurons are also subject of degeneration, which contributes to the cardinal symptoms tremor, rigor and akinesia (Rommelfanger and Weinshenker 2007). The parkinsonian symptoms start if 70% of the substantia nigra pars compacta neurons which project to the striatum get lost. The remaining nigrostriatal neurons are apparently able to compensate a loss by increasing the synthesis and release of dopamine (DA). A higher postsynaptic DA receptor sensitivity also contributes to this mechanism of compensation (Rinne 1982).

How leads the degeneration of dopaminergic neurons to the clinical symptoms? The corpus striatum contains GABA-neurons and a smaller number of cholinergic interneurons which are normally blocked by dopamine. In the case of PD the cholinergic neurons are disinhibited triggering an imbalance between cholinergic and dopaminergic neurotransmission. This is a fundamental step to the clinical symptomatology (Lusis 1997).

The picture is even more complicated if you consider the complex wiring of the extrapyramidal motoric basal ganglia, as a key controller of selection and processing of currently required motor and higher integrative non-motor operation schemes. In the same time, currently not required activation patterns are suppressed. The basal ganglia can be understood as complex loop going from the cortex over the basal ganglia to the thalamus and back to the cortex (Fig. 2).

Let us have a look on the function and the components of the basal ganglia in normal and pathological conditions to assess the therapeutical potential of amantadine. From the whole cortex glutamatergic neurons are going to the striatum which is the entry nucleus of the basal ganglia. There, they activate GABAergic and cholinergic neurons. The further way to the thalamus is complicated and comprises a direct and indirect pathway (Schmidt 1995). The direct pathway is excitatory while the indirect pathway is inhibitory.

The direct pathway involves GABAergic neurons of the striatum the globus pallidus medialis (Gpm) and the substantia nigra pars reticularis (Snpr). GABA neurons of the striatum are activated through DA coming from fibres of the substantia nigra pars compacta (Snpc) , activating D1-receptors.

This GABAergic projection from the striatum to a GABAergic projection from the Gpm to the motor thalamus leads to a disinhibition of motor thalamic glutamatergic neurons, and thus facilitates movement. The same molecular mechanism and neuronal architecture is true for GABA projections of the striatum to the Snpr, which also triggers activation of the motor thalamus.

The indirect connection is a little bit more complicated. Some GABA neurons of the striatum are inhibited through D2-receptors in the presence of DA, this is the case if the first pathway is active. If DA levels decline, the GABA neurons which are responsible for the second pathway are activated. These GABA neurons project to the globus pallidus lateralis, where they inhibit GABA-type neurons projecting to the subthalamic nucleus (STN). The inhibition of the inhibition leads again to the disinhibition of downstream located neurons, which are glutamatergic. The STN depicts a regulation link of the activities from GABA neurons of both Gpm and Snpr, which means that increased firing leads to enhanced GABA-ergic transmission and in fact weakens the activity of the motor thalamus.

In the pathological absence of DA, the activity of GABA neurons of the direct pathway is reduced and the GABA neurons of the indirect pathway are enhanced (McAuley 2003). The outcoming filterfunction of sensorimotoric signalling to the cortex is increased by a dampening of the motor thalamus. This results in rigor, tremor and akinesia which are the major symptoms of PD.

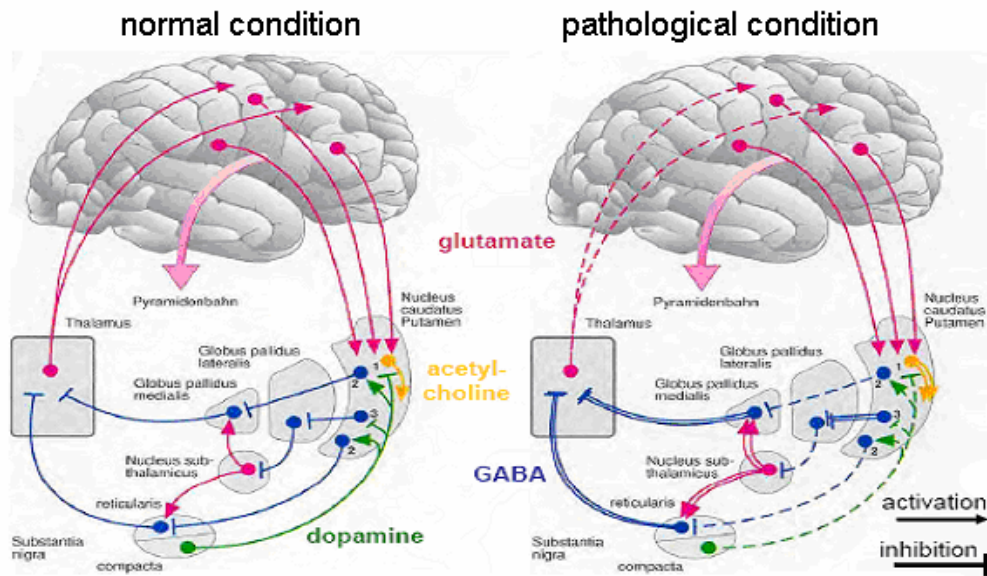


Fig. 2: extrapyramidal-motoric basal ganglia loop in healthy (left picture) and in case of Parkinson (right picture) arrow tips: activation; dotted lines: activity reduction; doubled lines: activity increase; glutamate: red; GABA: blue; dopamine: green; acetylcholine: yellow; 1, 2, 3: actions of dopamine and impaired functions in case of deficiency of dopamine

In literature amantadine is described as uncompetitive NMDAR antagonist (Kornhuber et al., 1991; Stoof et al. 1992; Blanpied, Clarke et al. 2005), which may explain its effect in PD. In the case of PD subthalamic glutamatergic efferents to Gpm and Snpr are disinhibited and push GABA neurons through NMDAR. This might explain why NMDAR blockers like amantadine and memantine reduce PD symptoms. In the case of mild symptoms it is therapeutically usefull to begin PD therapy with amantadine or memantine in combination with muscarine recptor antagonists. If this medication is not longer able to restrain the functional limitations of PD symptoms one may add a DA receptor agonist. If this first line therapy fails it is useful to add the currently most powerful weapon (-)-3,4-dihydroxyphenylalanine (levodopa) with decarboxylase-blockers. Levodopa can cross the blood-brain barrier and is intracellularly decarboxylated to DA, while the decarboxylase blocker remains in the periphery, thereby preventing an enzymatic transformation of levodopa to DA outside the brain. There a higher DA level is associated with unwanted side effects such as unstable blood pressure or cardiac side effects.

1.1.3 Dyskinesia in PD

Levodopa and DA agonists are the mainstay of pharmacological therapy for PD and are able to control PD symptoms adequately for a prolonged period of time. However, chronic therapy with these medications is often associated with the development of choreiform, involuntary movements called drug-induced dyskinesias (DID). They are defined as abnormal, excessive and involuntary movements. As the duration of dopaminergic treatment increases to a mean of 6 years, over two-third of patients will develop DID (Lim 2005).

DID represents a major source of disability and anxiety among the patients. Moreover, it acts as a dose limiting factor which prevents satisfactory control of PD symptoms. As described before, an abnormal lack of DA leads to hyperactivities of the output nuclei Gpm and Snr induced by STN leading to excessive inhibition of the motor thalamus and the cortex which in turn causes an akinetic crises and other parkinsonian features. Levodopa is hypothesized to normalize the direct and indirect striatal output pathways, thereby reducing Snr and Gpm overactivities.

The current state of the art models of DID suggest on the other hand that an excessive decrease in Snr and Gpm activities disinhibit the motor thalamus giving rise to an abnormal increase in cortical drive and hardly controllable choreiform motor movements (Papa et al. 1999). But what is responsible for such abnormal alterations? The most accepted hypothesis is nigro-striatal denervation, coupled with non-physiological dopaminergic stimulation. A chronic pulsatile stimulation of DA receptors leads to persistent changes in the basalganglia which in turn favours an abnormal pattern of discharges in the circuitry and consequently causes dyskinesia.

However, further studies indicate that things are not that simple, because of a variety of neurochemical and molecular factors contributing to DID. One group argues that development of DID is linked with the appearance of D3 receptor mRNA binding sites in the denervated caudate and putamen from which this receptor subtype is normally absent (Bordet et al. 1997) . GABA neurotransmission is also widely seen in the basal ganglia. There are also changes in this system due to DA depletion. Chronic non-intermittent levodopa therapy causing pulsatile DA stimulation is shown to cause up-regulation of GABA_A receptors. In post mortem samples Calon and Di Paolo (2002) have shown increased GABA_A receptors content in the Gpm in dyskinetic PD patients, compared to nondyskinetic patients.

1.1.4 N-methyl- D-aspartate receptors and glutamate in DID

1.1.4.1 The NMDA receptor

The N-methyl-D-aspartate receptor (NMDAR) is a specific type of ionotropic glutamate receptor often colocalized with DL- α -amino-3-hydroxy-5-methyl-4-isoxazolepropionic acid (AMPA) receptors in the brain. N-methyl-D-aspartate is a selective agonist binding to the NMDAR but not to other glutamate receptors.

NMDARs have unique properties, they are both ligand gated and voltage dependent. For the activation of the nonselective cation channel first glutamate and glycine must bind on NMDAR. As NMDARs are blocked with extracellular Mg^{2+} , little ionic current passes. After glutamate release AMPA channels are activated being a pore for Na^+ . If current flows through AMPA channels the membrane is depolarized. If glutamate release coincides with depolarisation sufficient to displace the Mg^{2+} ions from the NMDAR, a flow of Na^+ and small amounts of Ca^{2+} ions into the cell and K^+ out of the cell takes place (Bear 2001). This process plays a pivotal role in LTP, a process which is implicated in molecular learning processes like memory and pathologic processes like chronic pain and addiction.

The NMDAR consists of two NR1 and NR2 subunits forming a heterotetramer. There are eight splice variants of the NR1 subunit, but NR1-1a is the most abundantly expressed form. The NR2 subunit got also various isoforms termed NR2A through D. The NR1 subunits bind the coagonist glycine and NR2 subunits bind the neurotransmitter glutamate (Cull-Candy et al. 2001).

Antagonists of the NMDAR are used as anesthetics and have often hallucinogenic properties like ketamine and PCP, but there exist also others with therapeutic effects against neurodegenerative diseases like memantine and amantadine as well as anticraving therapeutics like acamprosate.

1.1.4.2 Glutamate receptor mediated mechanisms in DID

Glutamate is the main excitatory neurotransmitter in the basal ganglia circuitry. As dopaminergic denervation progresses the glutamatergic neurotransmission is thought to become overactive.

Attempts to suppress it with manipulation of common dopaminergic drugs often fail, leading to the exploration of alternative approaches. Glutamate receptor mediated mechanisms have been proposed as contributing factors in levodopa- related motor complications in animal models.

All glutamate receptor subtypes (NMDA, AMPA, Kainate and metabotropic) are found in the basal ganglia circuitry although NMDA receptors may play a key role in the development of DID. NMDA receptor binding was shown to be increased by 53% in the putamen of PD patients with motor fluctuations when compared to those without (Calon et al. 2003).

One major mechanism to improve dyskinesia could be the blockade of NMDARs, but the toxicity of clinically available glutamate antagonists generally precludes full characterisation of their antidyskinetic potential. As amantadine is a safe and widely used antiparkinsonian agent which is known to be an uncompetitive NMDA receptor blocker (Kornhuber et al., 1991; Stoof et al. 1992), its antidyskinetic potential has been evaluated in animal models as well as in human studies.

The group of Thomas Chase (Blanchet et al. 1998) used MPTP monkeys which showed choreiform and dystonic dyskinesia after a long-time of levodopa administration. When administered with a relatively low dose of levodopa, amantadine showed a total suppression of choreiform dyskinesia as well as a substantial reduction of dystonic dyskinesia. With a high dose of levodopa amantadine had a smaller but still significant effect on dyskinesia without worsening parkinsonian scores. The positive effects of levodopa also remained without being disturbed by NMDA receptor blockade.

In a double-blind, placebo controlled, cross-over study Verhagen, L. and colleagues (Verhagen Metman et al. 1998) wanted to assess the anti dyskinetic potential of amantadine in 18 patients. In the 14 patients completing this trial, amantadine reduced dyskinesia severity by 60% compared to placebo, without altering the antiparkinsonian effect of levodopa. It is unclear, if amantadine might be selective for a specific subunit of the NMDA receptor complex. Drugs which are in development selectively targeting certain subunits are supposed to give even greater benefits to the patients without increasing adverse effects. However, based on the current results, a large proportion of patients with advanced PD and motor complications can be expected to benefit from the addition of amantadine to their standard medications. Nevertheless, amantadine may have also side effects including nervousness, anxiety, agitation, insomnia and difficulty in concentrating.

1.2 Implications of the noradrenergic system in PD

The main hallmark in PD is the loss of nigrostriatal DA neurons leading to the well known symptoms akinesia, tremor and rigor. As described before, the gold standard in therapy is levodopa which ameliorates those motor symptoms. It could have been shown that several of the symptoms of PD, mostly those which appear in the later stages, do not respond satisfactorily to levodopa treatment. Symptoms like cognitive disorders, postural instability, a frozen gait and autonomic dysfunction are believed to be rather of noradrenergic than dopaminergic nature. Post-mortem studies have shown that also noradrenergic neurotransmission is impaired in PD. There is a decrease in NA-levels combined with a neuronal loss in the locus coeruleus of patients with PD (Gesi et al. 2000). The site where NA nuclei are located is mainly the LC or A6 cell group and medullary nuclei designated as A1,2,A5 and A7 (Fig. 3). The LC projections go to the whole neocortex and the limbic forebrain (amygdala, septum, hippocampus).

Cell groups from A1-A7 innervate mostly the septum and hypothalamus. In addition a descending pathway innervates the spinal cord which provides autonomic functions. The LC projections are widespread in the central nervous system and may have pervasive effects at diverse terminal regions such as the neocortex and limbic areas. These facts suggest the implication of the NA system in several processes such as motor function, learning, memory, mood and autonomic functions which are all together impaired in PD.

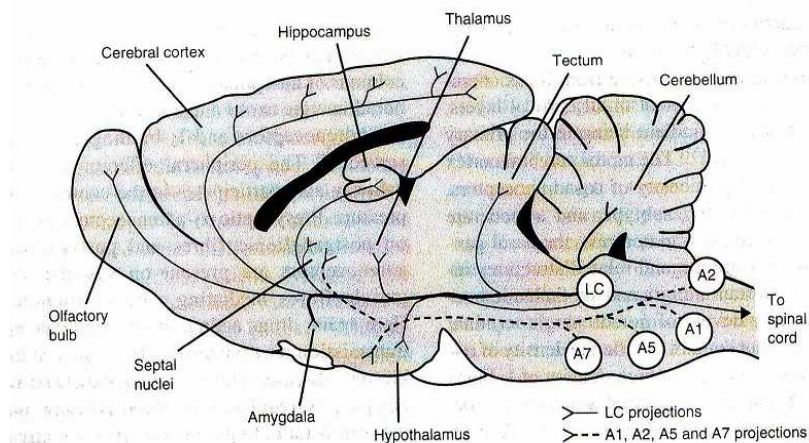


Fig. 3: Noradrenergic nuclei and their projections in the rat brain. LC = locus coeruleus

A large body of evidence indicates that noradrenergic systems interact with dopaminergic systems in the brain. Electrophysiological findings suggest that LC neurons can stimulate nigral neurons. Noradrenergic neurons exert a tonic excitatory influence on SNc DA neurones since experimental lesions of the LC with neurotoxins decrease the release of DA in the rat

striatum as measured by microdialysis in vivo (Lategan et al. 1992). Thus, there is a rationale for pharmaceuticals enhancing central noradrenergic function. Studies have shown a possible neuroprotective effect of so called α_2 -adrenoceptor antagonists.

1.2.1 Noradrenergic α_2 autoreceptors

Alpha-2 receptors are located both post and presynaptically. The significance of presynaptic receptors is their ability to modulate transmitter release (Langer 1980). Presynaptic α_2 receptors are autoreceptors which are excited by NE released by the respective neuron. The autocrine activation of α_2 adrenoceptors inhibits NE release. Several possible mechanisms are supposed to be responsible for a diminution of NE release. The coupling of α_2 autoreceptors with a G_i -protein leads to an inhibition of adenylate cyclase, resulting in a decrease of intracellular cAMP and Ca^{2+} concentration. It attenuates the rate of Ca^{2+} entry through inhibition of voltage gated Ca^{2+} channels and inhibits thus vesicle fusion. A further activation and opening of K channels triggers hyperpolarisation of the neuron terminals. On the other hand autoreceptors of the β_2 subtype mediate facilitation of NE release due to stimulation of adenylate cyclase with a G_s protein, leading to an increase in cAMP and a subsequent increase in intracellular Ca^{2+} concentration.

The presence of presynaptic facilitatory and inhibitory adrenergic receptors on the same nerve terminals provide a fine-tuning control of stimulus-evoked NE release which could be influenced in favour of an increased NE release by α_2 adrenoceptor blockers like idazoxan or yohimbine (Langer 1980).

1.2.1.1 α_2 -adrenoceptor blockers in PD

In humans a parallel group, double blind, randomised, placebo controlled study showed, if single doses of 25 and 100ug/kg idazoxan were administrated, an improvement of the unified Parkinson's disease rating scale motor score (by 25%) in 15 patients with PD (Peyro-Saint-Paul et al. 1995). The most influenced symptom (50-70% improvement) was rigidity, while tremor was not responsive to the drug.

In a study on MPTP monkeys rendered dyskinetic by high doses of levodopa an antidyskinetic effect have been observed without compromising the antiparkinsonian efficacy of levodopa (Bezard et al. 1999). In a study on 18 patients with Parkinson's disease receiving long term

levodopa treatment, the severity of L-DOPA-induced dyskinesia improved after 20 mg idazoxan pretreatment, while there was no concomittant worsening in the antiparkinsonian response to levodopa (Rascol et al. 2001). The exact mechanism of action has yet to be elucidated. It could be hypotesized that α_2 -adrenoceptor blockers located on LC neurons, leading to activation of the LC-SNc pathway resulting in an enhanced compensatory activity of surviving DA neurons.

Although α_2 -adrenoceptor antagonists may provide some benefit to patients with PD, they also can induce several side effects. In the periphery they can mediate troublesome cardiovascular effects by enhancing sympathetic tone, leading to increased blood pressure and tachykardia. At the central level α_2 -adrenoceptor antagonists can promote anxiety states and increase vigilance. Long term clinical studies are necessary to assess the safety of α_2 -adrenoceptor antagonists in the treatment of PD.

1.3 Effects of amantadine on DA and NE neurotransmission

According to the previous paragraph, enhanced NE and DA transmission by means of pharmaceutical manipulation can help to relief parkinsonian symptoms. Therefore, already in the 1970s the effects of amantadine on DA/NA uptake and release were intensively examined. The literature contains evidence that amantadine may act by releasing catecholamines (Scatton et al. 1970, Spilker et al. 1974), or by inhibiting the neuronal uptake of catecholamines (Thornburg and Moore 1973, Fletcher and Redfern 1970).

In a recent study, the effect of amantadine on extracellular DA levels in the rat striatum was studied using an in vivo microdialysis (Takahashi et al. 1996). Amantadine was applied through dialysis probe for 20min. The extracellular DA content was increased in a dose dependent manner. The findings of this study suggest that amantadine might influence DA concentration by facilitating DA release from striatal dopaminergic nerve endings.

In a rat model of PD, levodopa derived extracellular striatal DA levels were measured by in vivo microdialysis after unilateral denervation by 6-hydroxydopamine (Arai et al. 2003). After DA levels became stable all rats were injected with the decarboxylase inhibitor benserazide and divided into three groups and amantadine 10 or 30mg/kg, or vehicle was administered 15min prior to levodopa injection (50 mg/kg, 30 min after benserazide injection). A single dose of

levodopa given to the 6-OHDA-lesioned rats increased the DA levels to 286 fmol/sample at 80 min after levodopa administration. Pre-treatment with amantadine led to a higher value of 388 fmol/sample at 100 min in amantadine 10mg/kg group. The highest level was obtained in the 30mg/kg group with 670 fmol/sample. This is the first experimental study which exhibits the effect of amantadine on the metabolism of exogenous L-DOPA in rats with dopaminergic denervation.

In an earlier study Farnebo and colleagues (Farnebo et al. 1971) wanted to assess the DA and NA releasing action of amantadine in the central and peripheral nervous system. In biochemical superfusion experiments of tissues from untreated rats they studied the effect of amantadine. [³H]NA uptake was studied in isolated irides and slices of the cerebral cortex and the [³H]DA uptake in neostriatal slices. The irides were superfused after incubation with [³H]NA for 30 min and then electrically stimulated with biphasic pulses. The tritium efflux was higher if 10 µM amantadine was present in the buffer. Neostriatal slices were superfused after incubation with [³H]-DA for 40 min and then stimulated for 2 min. In this case there is also a higher tritium efflux in the presence of 10 µM amantadine.

In functional experiments rats with a 6-hydroxydopamine-induced unilateral degeneration of nigrostriatal DA neurons were treated with 50mg/kg amantadine. In these rats supersensitivity of DA receptors can be observed on the denervated site; DA receptor stimulating agents such as apomorphine increase the DA receptor activity preferentially on the denervated side forcing the rat to rotate to the intact side (Marshall and Ungerstedt 1977). In contrast, DA releasing agents, such as amphetamine only increase DA receptor activity on the intact side forcing the rats to rotate to the denervated side (Fig. 4, Ungerstedt, 1971).

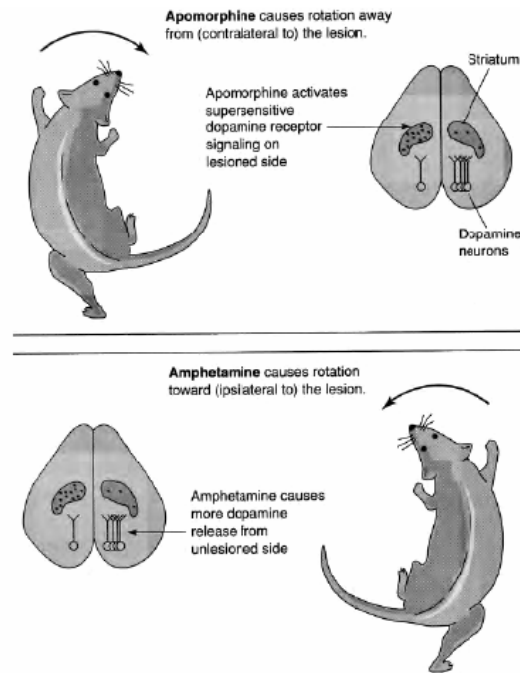


Fig. 4: Rotational behaviour of rats with unilateral degenerated nigrostriatal DA neurons induced by 6-OH dopamine. Apomorphine causes rotation away from the lesion due to activation of supersensitive dopamine receptor signalling on the lesioned side. Amphetamine causes rotation toward the lesion due to enhanced dopamine release from the unlesioned side (Ungerstedt, 1971).

Amantadine made the rats turn to the lesioned site. This fact, together with the previous superfusion experiments, suggested that amantadine is about 25-50 times less potent a releaser than amphetamine. Amphetamine exerts its action through the closely related monoamine transporters, dopamine and noradrenaline transporter. If amantadine acts via monoamine transporters, remains to be determined.

1.4 The noradrenaline transporter

The neurotransmitter NA, released from noradrenergic neurons of the peripheral or central nervous system is a prominent chemical messenger in both systems. The NA transporter (NAT) contributes to the termination of action of NA in the synaptic cleft by rapid removal through reuptake into the cytoplasm (Iversen 1971; Trendelenburg 1991). The NAT not only regulates the longevity of NA in the synapse but also plays a key role in maintaining the presynaptic and postsynaptic homeostasis. NET exerts a fine regulated control over NA-mediated behavioural and physiological effects including mood, depression, cognition, regulation of blood pressure and heart rate.

Pathomechanisms associated with the NAT e.g feeding disturbances and depression exhibit the NAT as a useful target for therapeutically used drugs.

1.4.1 NAT Structure and Function

Na^+ and Cl^- are the two critical ions involved in substrate transport by the NET. Br^- is the only other ion that can partially mimic the function of Cl^- . Other monovalent cations than Na^+ are not able to take over its unique role (Friedrich and Bonisch 1986). The Na^+ gradient based on a high Na^+ concentration outside and a low Na^+ concentration inside the neuron is the main driving force across the plasma membrane providing the transport direction from the outside to the inside. In addition K^+ is creating a negative membrane potential which contributes to the translocation mechanism. Both ion gradients are maintained by the key ion pump Na^+/K^+ -ATPase, which can be blocked by e.g ouabain leading to a suppression of NA uptake.

The group of H.Bönisch is suggesting a transport model based on a single centre gated pore mechanism with alternating access of the solute to the binding site (Bonisch 1998). In this model the empty and mobile carrier is loosing his mobility by first binding the co-substrate Na^+ . Subsequently, the substrate NA and the cosubstrate Cl^- are bound resulting in a regain of mobility. After translocation has finished by dissociation of substrate and co-substrates, the carrier is returning in its unloaded state to execute a new cycle (Fig. 5). The model proposes that NA is translocated as positively charged NA^+ and coupling of NA^+ transport with Na^+ and Cl^- occurs at a stoichiometry of $1\text{NA}^+:1\text{Na}^+:1\text{Cl}^-$ (Piffl et al. 1997).

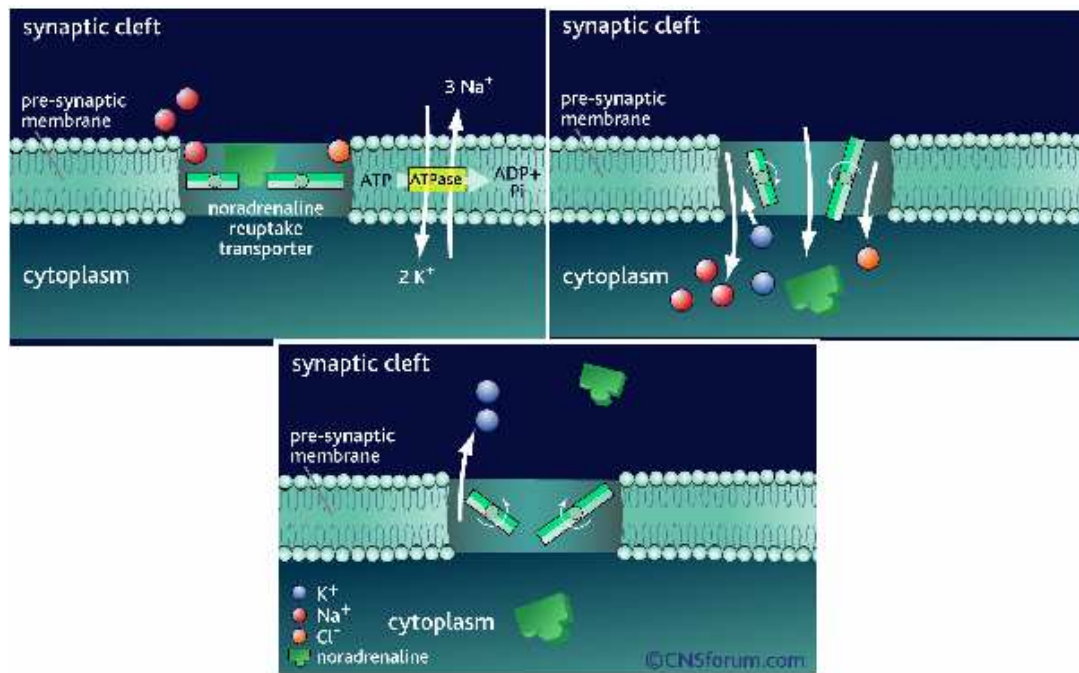


Fig . 5: Mechanism of noradrenaline transport. The action of noradrenaline at the synapse is terminated by its re-uptake across the pre-synaptic membrane. This is an energy dependent process. Sodium/potassium ATPases use energy from ATP hydrolysis to create a concentration gradient of ions across the pre-synaptic membrane that drives the opening of the transporter and co-transport of 1 sodium and 1 chloride ion and 1 molecule noradrenaline from the synaptic cleft. Potassium ions binding to the transporter enable it to return to the outward position. Release of the potassium ions into the synaptic cleft equilibrates the ionic gradient across the pre-synaptic membrane. The noradrenaline re-uptake transporter is then available to bind another noradrenaline molecule for re-uptake (www.cnsforum.com/imagebank/item/Rcpt_sys_N_reup_5/default.aspx).

The NAT, the DA transporter and the serotonin transporter belong to the family of Na⁺/Cl⁻ dependent monoamine transporters (Amara 1992). The cloned human NAT cDNA is an 1857 base pair open reading frame, predicting a protein of 617 amino acids with a mass of approximately 69 kDa (Pacholczyk et al. 1991). The hNAT protein consists of 12 putative transmembrane domains (TMs), each of 18-25 amino acids in length (Fig. 6). The amino and carboxy termini are both located in the cytoplasmic side. The large extracellular loop between TM3 and TM4 has several potential N-glycosylation sites. Glycosylation is strongly involved in cell surface expression, e.g. a fully glycosylated NAT protein has a greater likelihood of being expressed on the cell surface than a poorly glycosylated protein (Melikian et al. 1996). In addition to glycosylation sites, there are sites for potential phosphorylation by protein kinase C and casein kinase 2 within the intracellular part of the transporter. Experiments using chimera constructs between NAT and DAT suggesting that regions from the amino-terminal through the first five TMs are likely to be involved in the uptake process and ionic dependence, whereas the region from TM4 to TM8 is involved in substrate translocation (Buck and Amara 1994). Regions between TMs 6-8 are postulated to determine tricyclic antidepressant binding and cocaine interactions.

The large extracellular loop also contains two cysteine residues conserved among all members of the family suggesting to play a role in a functional transporter conformation.

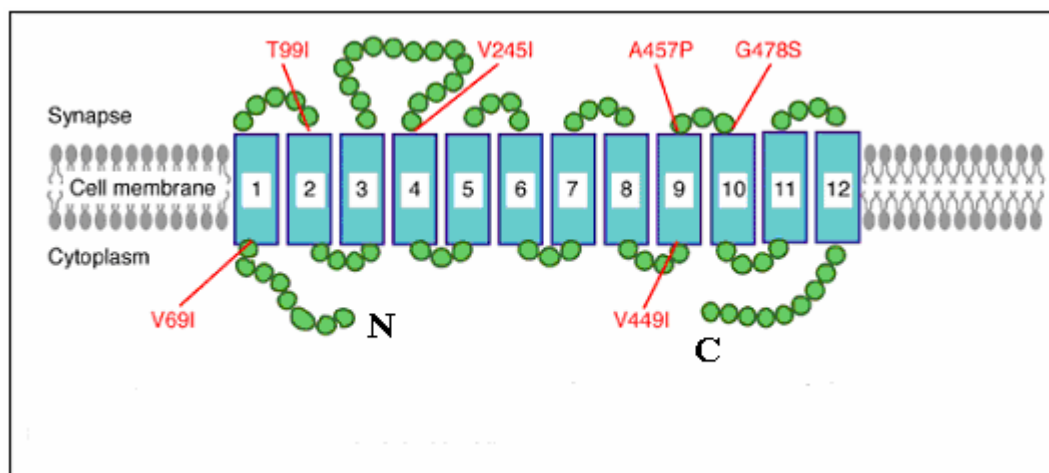


Fig.6: Schematic presentation of the hNAT viewed from the front. The typical hNAT has 12 transmembrane spanning domains. The amino and carboxyterminal domain lies in the cytoplasm. Five loops are located intracellularly and six loops extracellularly. The first five TMs are involved in the uptake process, whereas the region from TM4 to TM8 is involved in translocation (http://journals.cambridge.org/fulltext_content/ERM/ERM3_29/S1462399401003878sup004.htm).

1.4.2 Tissue expression

NAT mRNA expression is mainly located in the regions where noradrenergic pathways are present, respectively the LC complex in the dorsal pons, especially in the nucleus LC proper as it is revealed by [^3H]nisoxetine binding (Smith et al. 2006). [^3H]nisoxetine is a high affinity NAT inhibitor used as radioligand. NAT mRNA is additionally expressed in ensemble with dopamine- β -hydroxylase mRNA, which is a further marker for NAT expression patterns, in the lateral tegmentum of the medulla and pons (Eymin et al. 1995). All these regions inclose most of the noradrenergic cell bodies in the central nervous system. Interestingly, moderate concentrations of [^3H] nisoxetine binding in a serotonergic cell body region, the dorsal raphe nucleus have also been reported in rats. This illustrates the interconnections of the central noradrenergic and serotonergic neuronal systems.

Arising noradrenergic neurons originating from the locus coeruleus, project to many different brain regions and may thus influence complex neural pathways involved in autonomic and neuroendocrinal regulation, arousal, attention and affective behaviours like emotion and depression. In the periphery a NAT expression can be observed in the placenta the adrenal medulla and in sympathetic ganglia.

The NAT protein is expressed on noradrenergic cell bodies, dendrites and axons but not directly in the active zone of the synapse but more laterally (Schroeter et al. 2000). This has been demonstrated for the closely related DAT too.

1.4.3 Regulation of NAT function

NAT function can be regulated in several ways. It may be acutely or chronically depending on the stimulus. It may be due to changes in gene transcription, posttranslational modifications such as phosphorylation, protein trafficking, cytoskeleton interactions and oligomerization (Zahniser and Doolen 2001). A long term change may be due to long-term blockade e.g NAT inhibiting antidepressants. Long term application of desipramine was shown to produce up-regulation of NAT mRNA in the rat locus coeruleus.

In contrast phorbol-ester mediated activation of PKC, whose regulation among monoamine transporters seems to be universal, leads to phosphorylation of NAT. This in turn triggers its rapid internalisation into the cytoplasm from the plasma membrane. Reduced surface expression of NAT is the primary mechanism contributing to PKC-induced decrease in NAT activity (Bonisch et al. 1998).

Also neurotransmitters like acetylcholine are altering transporter function by reducing K_m but not V_{max} , thus decreasing NA uptake. Angiotensin II affects blood pressure in the sympathetic nervous system which uses NA as neurotransmitter and is interacting with the NAT. A long term Angiotensin II triggered activation of the AT1 receptor induces an up-regulation of NAT mRNA through activation of the Ras-Raf-MAP kinase (Lu et al. 1996). Short term Angiotensin II exposure leads to an increase of NA uptake by a posttranscriptional event inducing a rapid increase in NAT surface expression. The process of NAT movement from the plasma membrane is supported by a close localization of synaptic vesicle pools and proteins like syntaxin1 and SNAREs with the NAT.

1.4.4 NAT inhibitors

In the nanomolar range the NAT is inhibited by various antidepressants (ADs) such as the tricyclic ADs nortryptiline and the ADs reboxetine, nisoxetine and atomoxetine. Among the tricyclics desipramine is the most selective one whereas the most selective drug under all

mentioned is reboxetine (Kaspar et al. 2000). The psychostimulant cocaine and its phenyltropane analogue RTI-55 are also blocking the NAT but are not so selective as they additionally block the DAT and the SERT (Olivier et al. 2000).

The high-affinity drugs desipramine and nisooxetine are experimentally used as radioligands thus providing density of transporter sites in various tissues. Different studies indicate that NAT inhibitors bind to a site at the NAT which is not identical with the substrate recognition site but may overlap with it. However, the drug-binding site and the mechanism of this inhibition are poorly understood. It is suggested that all blockers have in common that they are directly locking the gate, preventing a conformational change, thus inhibiting substrate transport (Zhou et al. 2007).

1.5 The dopamine transporter

The DA transporter (DAT) is an integral membrane protein in dopaminergic cells that removes DA from the synaptic cleft and reuptakes it into the presynapse where DA is then recycled and packed into vesicles in a clathrin dependent process. Because DAT is terminating the DA signal it plays a crucial role in DA related disorders like attention-deficit hyperactivity disorder, clinical depression, alcoholism and cocaine addiction (Sharp et al. 2009; van der Zwaluw et al. 2009).

The DA uptake sites interact with MPP⁺, the active metabolite of the parkinsonism inducing drug MPTP, as they represent the preferred port of entry into the dopaminergic cell. Besides of pharmacology, the decisive role of DAT was finally revealed by its knockout in mice, triggering behaviour similar to ADHD in human.

1.5.1 Function and mechanism of dopamine transport

DAT is a symporter that moves one DA molecule and two Na⁺ in presence of one Cl⁻ across the cell membrane by coupling the movement to the energetically favourable movement of sodium ions along the concentration gradient into the cell (Fig. 7). In two independent studies a fixed binding order of Na⁺ before DA was observed (McElvain and Schenk 1992). If all three binding partners are present, the protein undergoes a conformational change eliciting the

translocation step. The lower affinity of DA for the DAT at higher $[K^+]/[Na^+]$ ratios in the intracellular fluid may favour the dissociation of DA from the DAT on the inside. The mechanism for uptake of DA and other biogenic amines is controlled by the transmembranal gradient of Na^+ and breaks down in a medium in which Na^+ is iso-osmotically replaced with sucrose, choline or lithium (Syringas et al. 2000). Substitution of Cl^- with other anions causes also a markedly reduced high-affinity uptake.

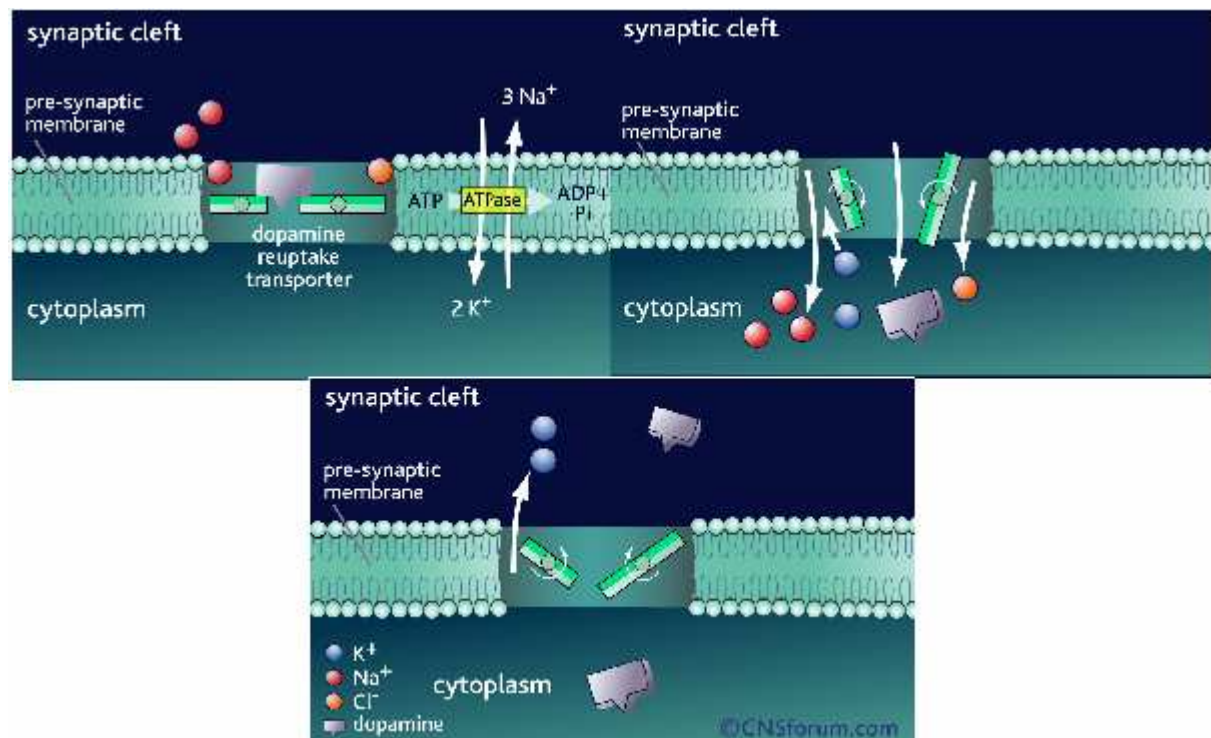


Fig. 7: Mechanism of dopamine transport. The action of dopamine at the synapse is terminated by its re-uptake across the pre-synaptic membrane. This is an energy dependent process. Sodium/potassium ATPases use energy from ATP hydrolysis to create a concentration gradient of ions across the pre-synaptic membrane that drives the opening of the transporter and co-transport of 2 sodium and 1 chloride ions and 1 molecule dopamine from the synaptic cleft. Potassium ions binding to the transporter enable it to return to the outward position. Release of the potassium ions into the synaptic cleft equilibrates the ionic gradient across the pre-synaptic membrane. The dopamine re-uptake transporter is then available to bind another dopamine molecule for re-uptake (www.cnsforum.com/imagebank/item/rcpt_sys_DA_reup/default.aspx).

1.5.2 Protein Structure

The human DAT protein has an estimated size of 68-70 KDa and a 92% overall identity with the rat. Its homology with the human NET is 66% followed by 46% with the serotonin and 42% with the GABA transporter. The DAT is part of a family of Na^+/Cl^- -dependent transporters which is debilitated in its function without the correct ratio of Na^+Cl^-/K^+ (Nelson 1998). In biochemical and bioinformatical approaches the structure has been predicted with 12

stretches of 20-24 hydrophobic amino acid residues that likely represent membrane spanning domains (Fig. 8). The amino and carboxyterminal domain is supposed to be into the cytoplasm. The proposed model predicts five intracellular and six extracellular loops between the TMs. N-glycosylation of the transporter occurs between TM3 and TM4. Two co-ordinating residues in the large extracellular loop and in the loop between Tm7 and TM8 has been found which provide spatial proximity between the loops (Vaughan 1995; Volz and Schenk 2005). The transporter is also intracellularly modified by protein kinase C (third intracellular loop), cAMP-dependant protein kinase (near the amino terminal domain) and Ca^{2+} -calmodulin-dependent kinase (near the carboxyterminal domain). TM2 and TM9 display two leucine zipper motifs, structural features that are normally present in DNA-binding proteins mediating protein-protein interactions and might be involved in structural organisation of the transporter. The substrate binding pocket lies between the second and fourth extracellular loop which are in spatial proximity due to histidine residues, building a Zn^{2+} coordination centre (Loland et al. 2002).

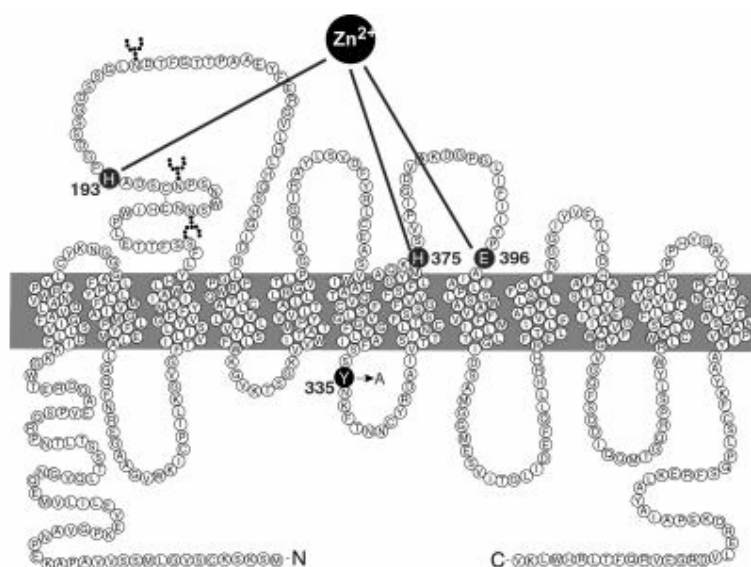


Fig. 8: Schematic presentation of the hDAT viewed from the front. The typical hDAT has 12 transmembrane spanning domains. The amino and carboxyterminal domain lies in the cytoplasm. Five loops are located intracellularly and six loops extracellularly. The substrate binding pocket lies within the second and fourth extracellular loop which are in spatial proximity due to histidine residues, building a Zn^{2+} coordination centre (Loland et al. 2002)

1.5.3 Uptake blockers

DAT is also the target for uptake blockers which are strictly speaking drugs which interact with the transporter and lock it in a conformation where no translocation in both directions is possible. One example is cocaine (Ravna et al. 2003). Under the action of cocaine more DA is available in the synapse (Fig. 9) and our reward system is overstimulated eliciting a pleasurable

feeling and reinforcement. Self administration experiments of cocaine, performed with rodents, show us the addictive potential of this substance.

1.5.4 Amphetamine like substances

All lipophilic and thus centrally active phenylethylamines are belonging to this group. A wide range of behavioural processes are affected: motor activity, aggression, sexual behaviour learning, memory and self administration are mostly stimulated, whereas sleep, digestion and spermatogenesis are suppressed. Amphetamine-like drugs increase the action of both DA and noradrenaline in the synapse but are dependent of an intact system of DA or NA neurons.

Amphetamine activity involves several crucial steps (Fig. 9) (Gainetdinov et al. 2002; Sulzer et al. 2005). First it enters into the neuron by DAT. Then it penetrates into vesicles via the vesicular monoamine transporter 2 (VMAT2) or diffusion and disrupt the vesicular pH gradient, which leads to redistribution of vesicular stores of DA into the cytoplasm. Amphetamine subsequently reverses the DAT in a process called exchange diffusion. This in turn results in a massive outflow of DA to the extracellular space. Additionally amphetamine inhibits the monoamine oxidase, giving rise to a higher level of non degraded intracellular DA. This results in a raise of DA in the synaptic cleft, which is subsequently released in higher doses than under normal conditions. In the presence of DAT blockers amphetamine is not able to reverse the action of the DAT. The abusing potential is high and neurotoxic effects were demonstrated, especially for methamphetamine.

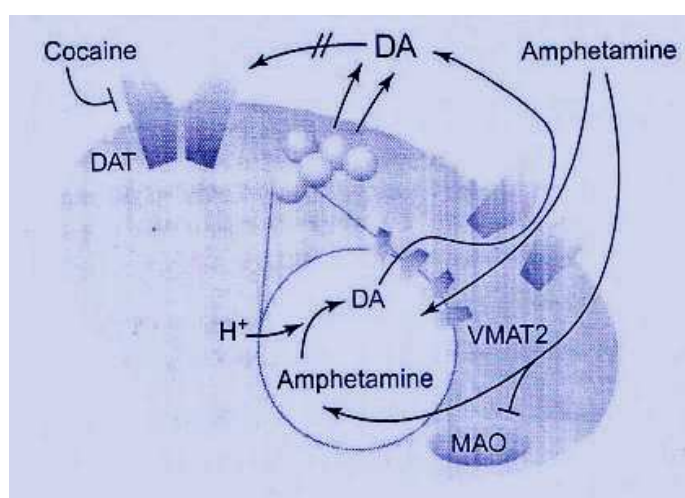


Fig. 9: Schematic presentation of cocaine and amphetamine action. Cocaine blocks the DAT thus inhibiting DA reuptake. Amphetamine action involves several crucial steps: entry into the neuron and disruption of vesicular pH gradient. Reversal of

DAT causes massive outflow of DA by exchange diffusion. Additional inhibition of MAO causes a rise in intracellular non degraded DA (Gainetdinov et al. 2002).

As DAT and NAT are electrogenic transporters binding of a transporter substrate will induce ion currents whereas an inhibitor will attenuate ion currents. This interplay can be studied by patch clamp recordings (Galli et al. 1995, Sitte et al., 1998; Khoshbouei et al. 2003).

1.6 Patch clamp

Patch clamp is a revolutionary method developed by the German neuroscientists Bert Sakmann and Erwin Neher (Neher and Sakmann, 1976). In 1991 they had been awarded the Nobel Prize. Patch clamping enables one to record ionic currents through single channels or the whole cell. This technique is based on a simple idea. A glass pipette with a very small opening is gently lowered onto the membrane of a neuron. The pipette contains an Ag/AgCl electrode which is connected to an operation amplifier, as well as a pipette solution corresponding to the intracellular fluid (Fig. 10). The reference electrode must be placed into the bath solution. The aim is to form a tight seal between the underlying patch of membrane and the walls of the electrode. It is named Giga-seal so because of its high electrical resistance $> 10^9$ Ohm.

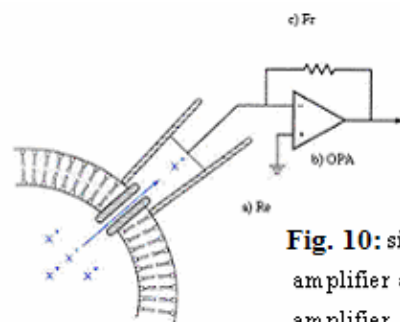


Fig. 10: simplified diagram of a patch-clamp amplifier a) reference electrode, b) operation amplifier, c) feedback resistance

After forming the Giga-seal the experimentator sucks on a tube connected with the pipette to break through the membrane. Now the whole cell recording mode is produced (Figure 10). The interior of the pipette becomes continuous with the cytoplasm of the cell. This mode allows measurements of electrical potentials and currents from the entire cell. It allows perfusion with different substances to investigate the behaviour of the whole cell.

There are also two other variants which are based on the finding if once there is a tight seal one can pull away the membrane with its intracellular surface exposed. This arrangement is called

the inside-out patch recording configuration. It allows measuring of single channel currents, making it possible to change medium to which the intracellular surface of the membrane is exposed. Channels that are activated by intracellular ligands like cAMP can then be studied through a range of ligand concentrations. On the other hand, if the pipette is torn away while it stays in the whole cell configuration, a membrane patch is produced having its extracellular surface exposed. This variant is called the outside-out configuration, which is optimal for examining the properties of an ion channel when it is protected from the outside environment, but not in contact with its usual environment. The same patch can now be perfused with different solutions e.g. neurotransmitter containing ones, and if the channel is intracellularly activated a dose response curve can then be studied.

2. Materials and methods

2.1 Cell culture

The cells used in my experiments are human embryonic kidney 293 cells grown in minimum essential medium with Earle's salts 1-glutamine, 10% heat-inactivated fetal bovine serum and 50 mg/l gentamicin on 60 or 100 mm tissue culture dishes (Falcon) at 37°C and 5% CO₂/95% air. The cells were either transiently or stably transfected with the human DAT, NAT or NMDA-receptor subtype NR1/2A. For the stable expression of hDAT and hNET in HEK cells the expression vector pRc/CMV was used as described previously (Piffl et al., 1996). The cell lines used were called 293D13 and 293N17. For most of the patch-clamp experiments and for all experiments on NMDA-receptor expressing cells the tetracycline-regulated expression system called T-RexTM was used which allowed expression of the proteins in an inducible manner.

2.1.1. Cells expressing the DAT or NAT in an inducible manner

T-RexTM is a tetracycline-regulated mammalian expression system that uses regulatory elements from the *E.coli* Tn10-encoded tetracycline (Tet) resistance operon (Fig.11).

Tetracycline regulation in the T-RexTM system is based on the binding of tetracycline to the Tet repressor and derepression of the promoter controlling expression of the gene of interest.

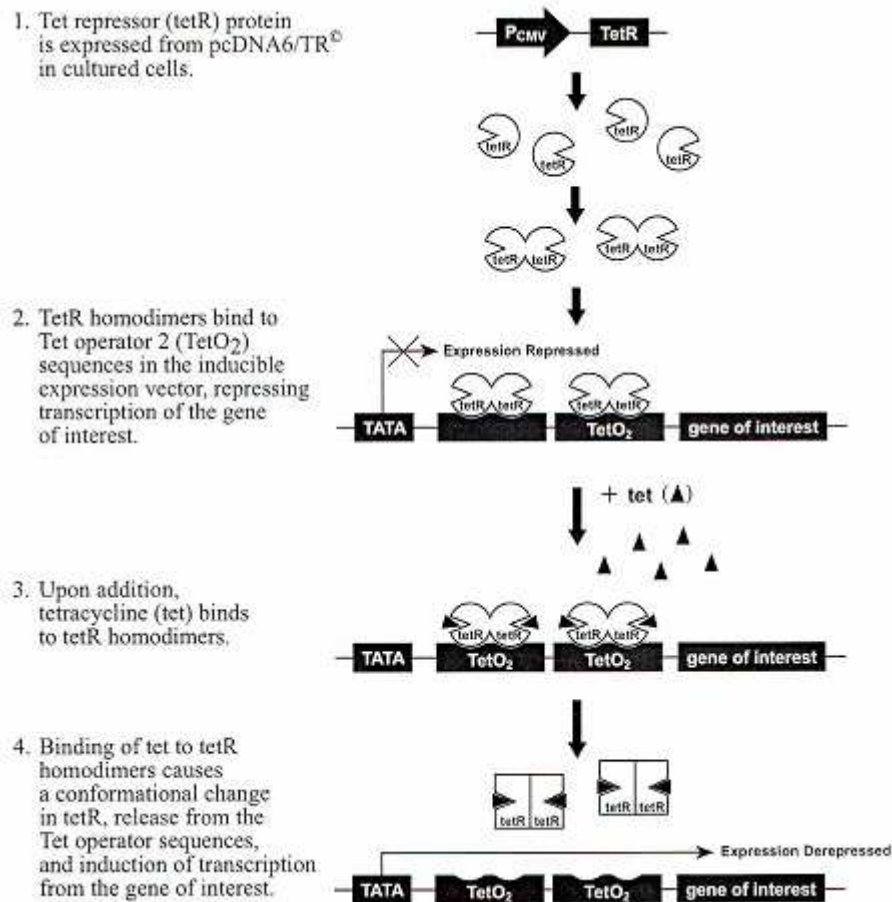


Fig.11: Repression of the Tet operator by the Tet repressor (1. and 2.) and induction of transcription by tetracycline (3. and 4.).

The main components of the T-RexTM system include (Fig.12):

- An inducible expression plasmid, pcDNA4/TO, for expression of a gene of interest under the control of the strong human cytomegalovirus immediate-early (CMV) promoter and two tetracycline operator 2(TetO₂)sites
- A regulatory plasmid, pcDNA6/TR[®], which encodes the Tet repressor (TetR) under the control of the human CMV promoter
- Tetracycline for inducing expression
- A control expression plasmid containing the *lacZ* gene, which when cotransfected with pcDNA6/TR[®], expresses β -galactosidase upon induction with tetracycline

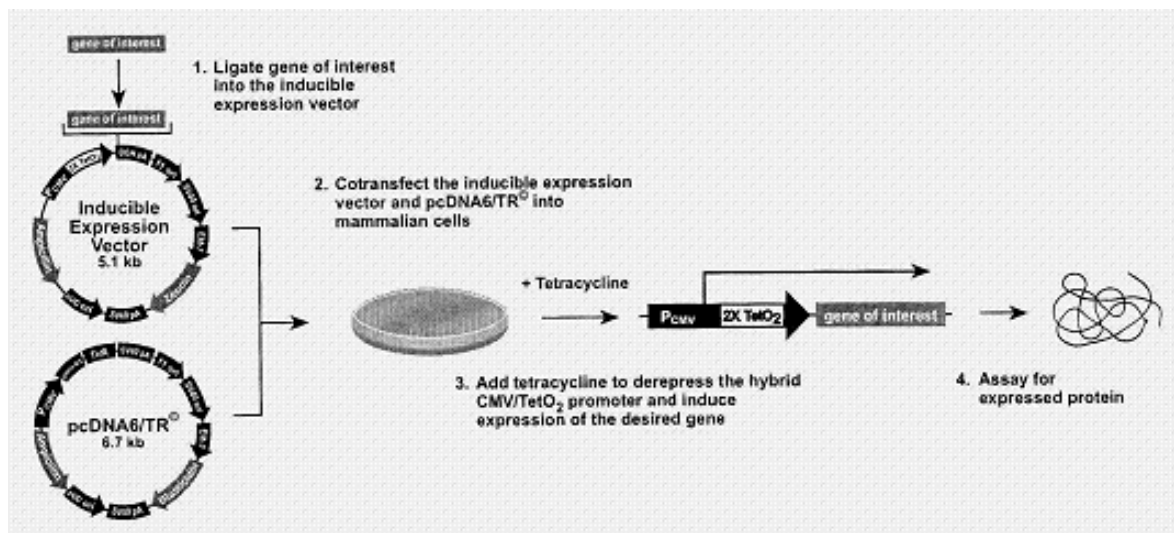


Fig. 12: Cloning of the gene of interest into the inducible expression vector and cotransfection with the regulatory plasmid pcDNA6/TR into mammalian cells. After transfection, cells are treated with tetracycline to derepress the hybrid CMV/TetO₂ promoter in the inducible expression vector and induce transcription of the gene of interest.

The cotransfection (see 2. in Fig.12) was done in two consecutive steps. In a first step HEK293 cells, or HEK293 cells stably expressing the hNAT after transfection with hNAT/pRc/CMV, were stably transfected with the regulatory plasmid pcDNA6/TR[®] which encodes the tetracycline repressor protein under the control of the human CMV promoter. The cell lines obtained from this first step were cells that we called 293/T-Rex and NAT/T-Rex. In a second step these cells were then stably transfected with the expression plasmid pcDNA4/TO inducibly expressing the transporter cDNA. For DAT expressing cells only 293/T-Rex were used, for NAT expressing cells both, 293/T-Rex and NAT/T-Rex, which should result in a particularly high expression level of NAT in case of NAT/T-Rex.

2.1.1.1. Transfection using calcium phosphate

Two million 293/T-Rex or NAT/T-Rex cells were plated into 100-mm diameter cell culture dishes one day before transfection. At the day of transfection, the medium was first changed. Six to seven hours later, 5 µg of hDAT/pcDNA4/TO - or hNAT/pcDNA4/TO-DNA in 450 µl of H₂O were mixed with 50 µl of 2.5M CaCl₂ and 500 µl of a solution containing 0.28 M NaCl, 50 mM 4-(2-hydroxyethyl)-1-piperazineethanesulfonic acid (pH 7.1) and 1.5 mM sodium phosphate and the total volume of 1 ml was added drop by drop to the 100-mm dish. In the next morning a glycerol shock was applied to boost the transfection yield: the medium containing Ca-phosphate precipitates was sucked off, the cells were shortly exposed to 1ml of 15%

glycerol in PBS, this solution was immediately diluted with 10ml PBS, sucked off and 10ml of new medium was added. One day after transfection, cells were split 1:4 and 1 day later selection of cells was executed with 0.3 g/l of zeocin (in presence of 5 mg/l of blasticidin) in the medium. After 2 to 3 weeks arising cell clones were transferred by sterile 200 µl Gilson plastic tips into 48 well plates, later grown up by consecutive splitting into 24- and 6-well plates and finally tested for uptake of [³H]DA in 24-well plates as described in chapter 2.3. Out of several cell clones displaying specific uptake the clones DAT/TO20, DAT/TO8, NAT/TO17 (obtained from 293/T-Rex) and N12/TO1 (obtained from NAT/T-Rex) were used for patch-clamp experiments.

2.1.2. Cell lines expressing the human NR1/2A NMDA receptor

I generated HEK-cells heterologously expressing a human NMDA receptor consisting of the subunits NR1 and NR2A. Since the expression of the NMDA receptor is cytotoxic I chose the inducible expression system T-RexTM. We received the cDNA of the hNR1 subunit inserted into the bluescript vector (Dr. Shigetada Nakanishi) and the cDNA of the hNR2A subunit (Dr. Antonio Ferrer-Montiel) in an unknown vector which we identified as pcDNAI by sequencing and bioinformatic alignment. A further cloning of the NR2A cDNA into the pcDNA4/TO vector appeared to be difficult because of unfavourable restriction sites. Therefore, I undertook to subclone the hNR1 into the pcDNA4/TO vector.

2.1.2.1. Subcloning of the NR1 subunit

The aim was to cut out the gene of the hNR1 subunit out of the bluescript cloning vector and insert it into the pcDNA4/TO expression vector. The length of NR1 is 2814 base pairs (bp), upstream from ATG there are 422 bp and downstream from TGA there are 1303 bp. This adds up to a cDNA of 4539 bp (Fig. 13), a little smaller than the gene with non-coding gene regions deposited in genbank (5137 bp). According to restriction sites in bluescript a cut with NotI and EcoRI was the most promising because pcDNA4/TO had NotI and EcoRI in the polylinker region allowing a directed insertion of NR1 with EcoRI ligation upstream and NotI ligation downstream. In order to obtain sufficient amounts of pHNR1 a maxiprep plasmid extraction was done followed by restriction digestions.

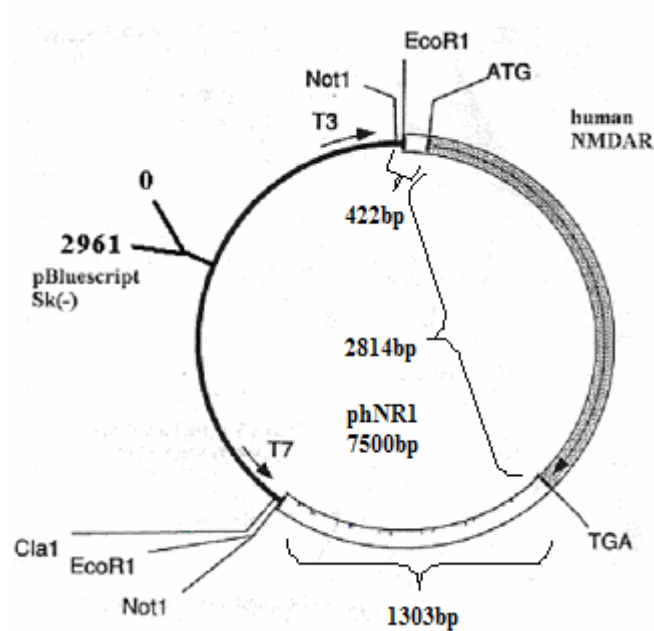


Fig. 13: Restriction map of the subunit NR1 in pBluescript SK(-), a plasmid phNR1 of 7500 bp received by Dr. Nakanishi. (Karp et al. 1993)

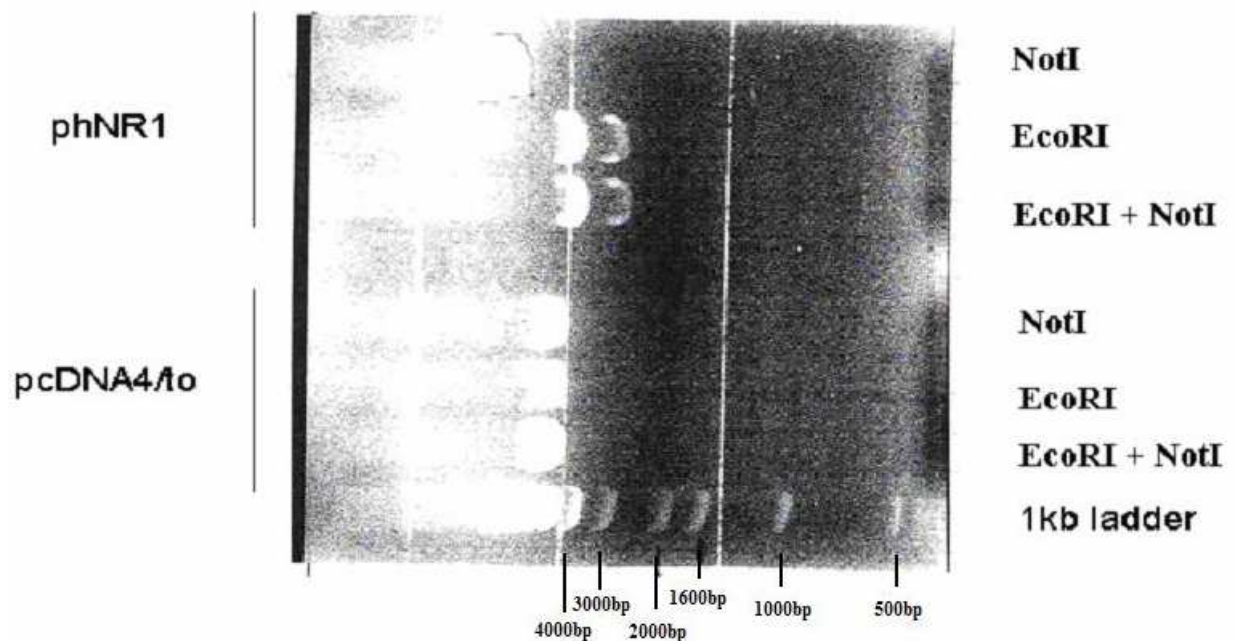


Fig. 14: Restriction digestion of phNR1 and pcDNA4/to with NOT1 and ECOR1

A cut with Not I linearized phNR1 or, due to the unclear visualization, left it unaffected (Fig. 14). Cutting with EcoRI+NotI or EcoRI alone resulted in the bigger insert (consistent with 4539bp) and the smaller vector (consistent with 2961bp), a similar pattern because of the vicinity of NotI and EcoRI upstream of NR1.

The same treatment of pcDNA4/TO resulted in one big fragment in each case, linearizing by the single cuts and cutting out just a few base pairs from the polylinker in case of EcoRI+ NotI.

Further restriction analysis using BclI on pHNR1 and BssHII on pcDNA4/TO should give information of the ability of NotI to cut pHNR1 and EcoRI and NotI to cut pcDNA4/TO (Fig. 15).

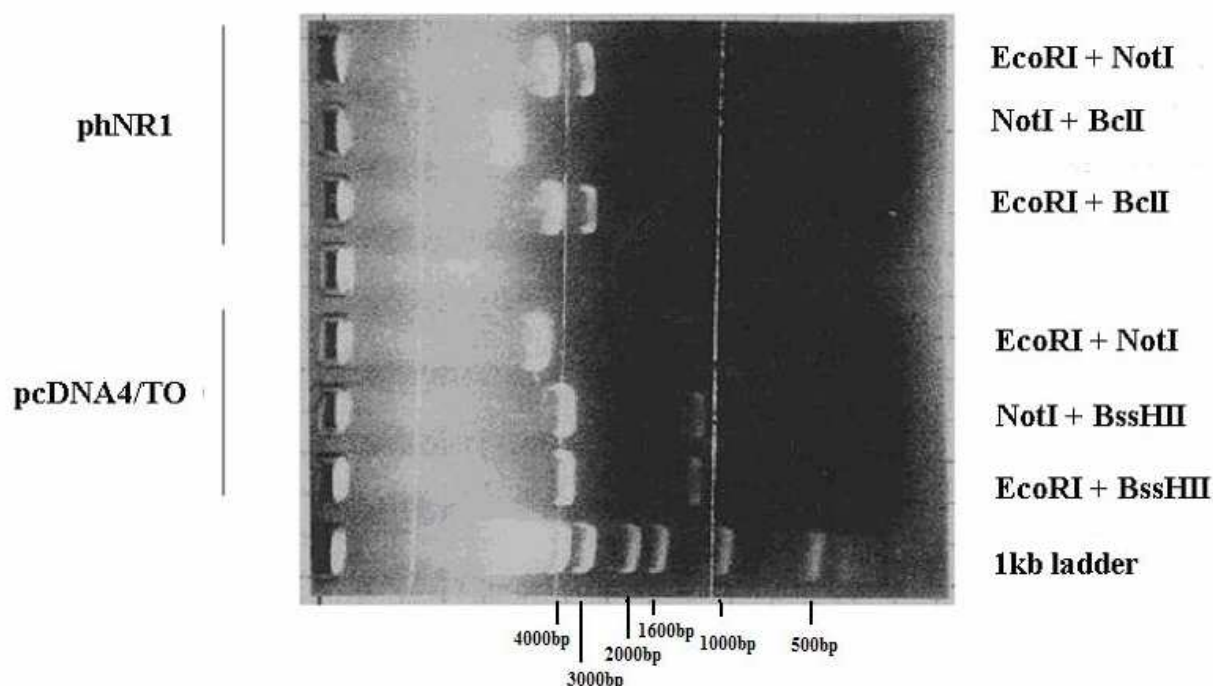


Fig. 15: Restriction digestion of pHNR1 and pcDNA4/to with different combinations of restriction enzymes.

The double cut by EcoRI+NotI of pHNR1 led again to vector (consistent with 2961bp) and insert (consistent with 4539bp). The double cut by NotI+BclI only linearized the construct (consistent with 7500pb), obviously BclI was not able to cut in our hands. In agreement with this interpretation, the double cut by EcoRI+BclI did not produce three fragments, but a similar result as EcoRI+NotI. The double cut of pcDNA4/TO (consistent with 5078 bp) by EcoRI+NotI presumably removed 27 bp from the polylinker resulting in one big fragment of about 5000 bp. A cut by NotI and BssHII, which is 1240 bp downstream of NotI, produced two fragments, the smaller about 1200 bp. The double cut EcoRI+BssHII resulted in similar fragments, the shorter one in agreement with the 1267 bp based on the restriction map of pcDNA4/TO. Thus, both EcoRI and NotI are able to open pcDNA4/TO.

Based on this information, the subcloning strategy was to cut out the NR1 from pHNR1 by EcoRI and ligate it into the pcDNA4/TO between EcoRI sites.

Therefore, 3 µg of phNR1 and 3 µg of pcDNA4/TO were cut by EcoRI (Fig.16).

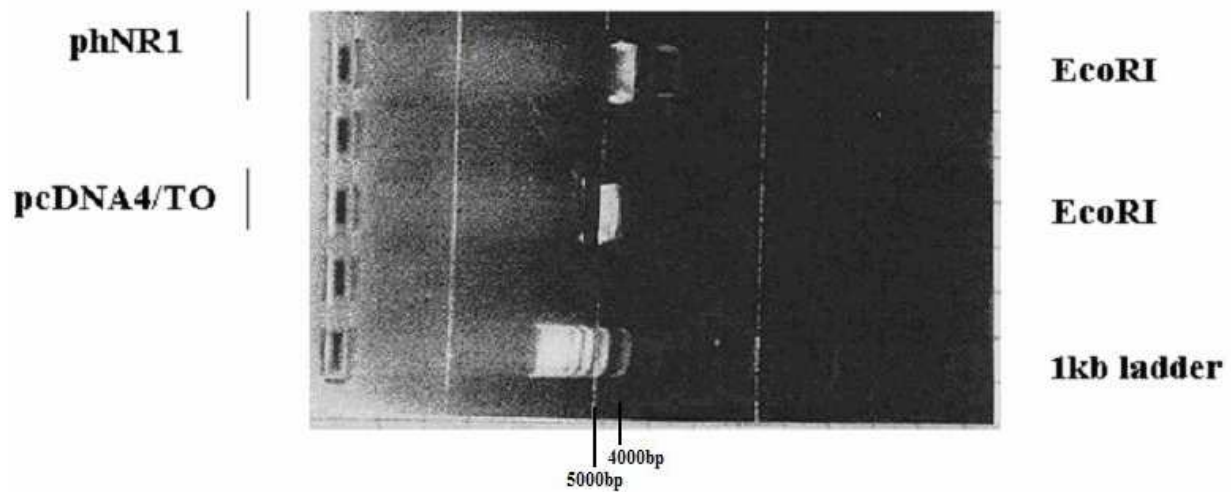


Fig. 16: Restriction digestion of phNR1 with Hind3 and EcoRI and pcDNA4/to with EcoRI

The resulting bands, about 4500 bp in case of phNR1 and 5000 bp in case of pcDNA4/TO (5078 pb according to Invitrogen), were extracted from the gel using the QIAquick gel extraction kit with a final extraction volume of 30 µl. This resulted in about $(3000 \times (4539/7500) \times 0.8) = 1452$ ng NR1 and in about $3000 \times 0.8 = 2400$ ng of linearized pcDNA4/TO, each in 30 µl, assuming an 80 % extraction yield of the kit. A 3:1 molar ratio of insert:vector was intended for ligation. Therefore, 50 ng of pcDNA4/TO required 134 ng of NR1 based on the formula $(\text{ng of vector} \times \text{kb size of insert}) / (\text{kb size of vector}) \times \text{molar ratio} = (50 \times 4539) / 5078 \times 3 = 134$ ng and the ligation was set up by mixing 2.8 µl of extracted insert 0,65 µl of extracted vector, 4.5 µl H₂O, 2 µl of 5x buffer, 10 µl of 2x ligase buffer and 1 µl of ligase (5 units/µl). After transformation of JM109 cells, 10 colonies were picked, minicultures grown and minipreps analysed for the subcloning product by HindIII digestion (Fig.17).

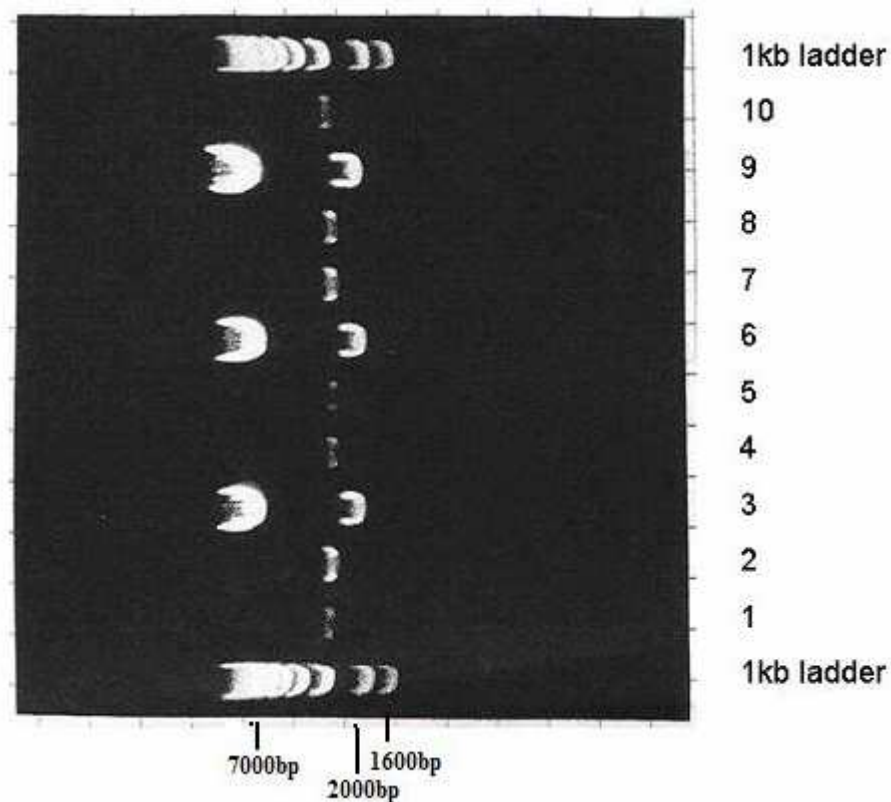


Fig. 17: Restriction digestion of minipreps with Hind III

After digestion with Hind III minipreps 3, 6 and 9 had 2 fragments which were about 7000 and 2400 bp long. Based on the restriction scheme in Fig.18 a fragment of 7206 = (5137-2968+5078-1020+979) bp together with a fragment of 2411 = (2968-598+1020-979) bp would indicate the right orientation, whereas 7407 = (2968-598+5078-1020+979) bp and 2210 = (5137-2968+1020-979) bp would indicated the wrong orientation. The slightly bigger fragment of about 2400 in miniprep 9 suggests a correct insertion in this case.

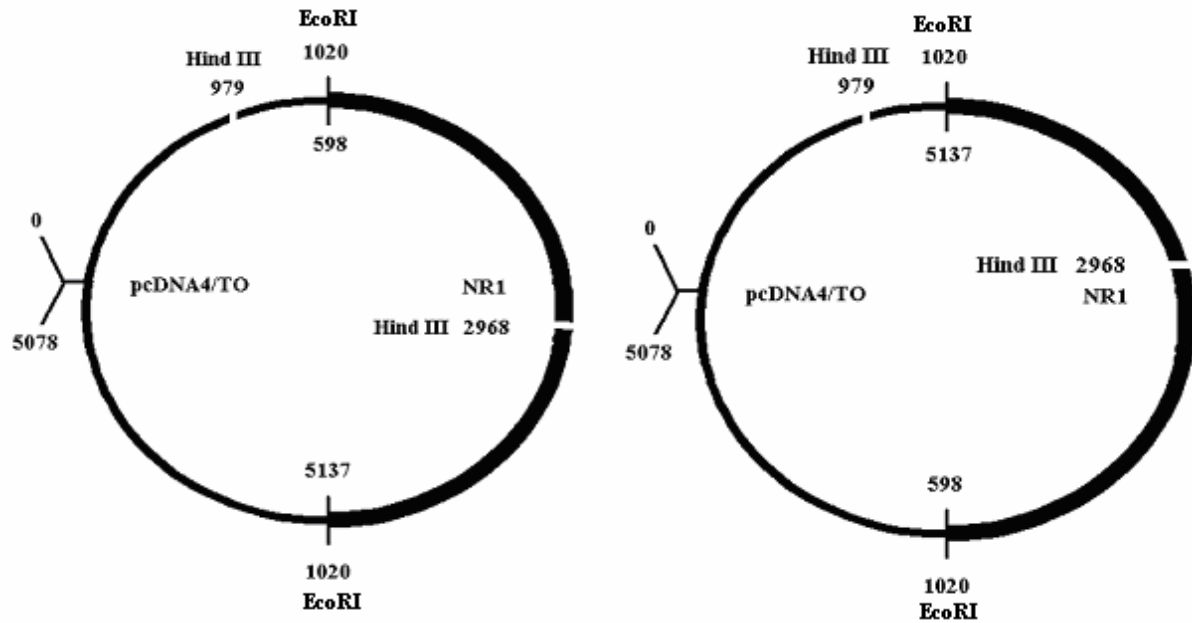


Fig. 18: Hind III cut of NR1/pcDNA4/TO with correct insertion on the left and the opposite insertion on the right. Outer numbers indicate positions of restriction sites within the vector, inner numbers the positions within the insert.

For clarification I decided to do another restriction digestion which produced 3 fragments using the enzyme BglII (Fig.19).

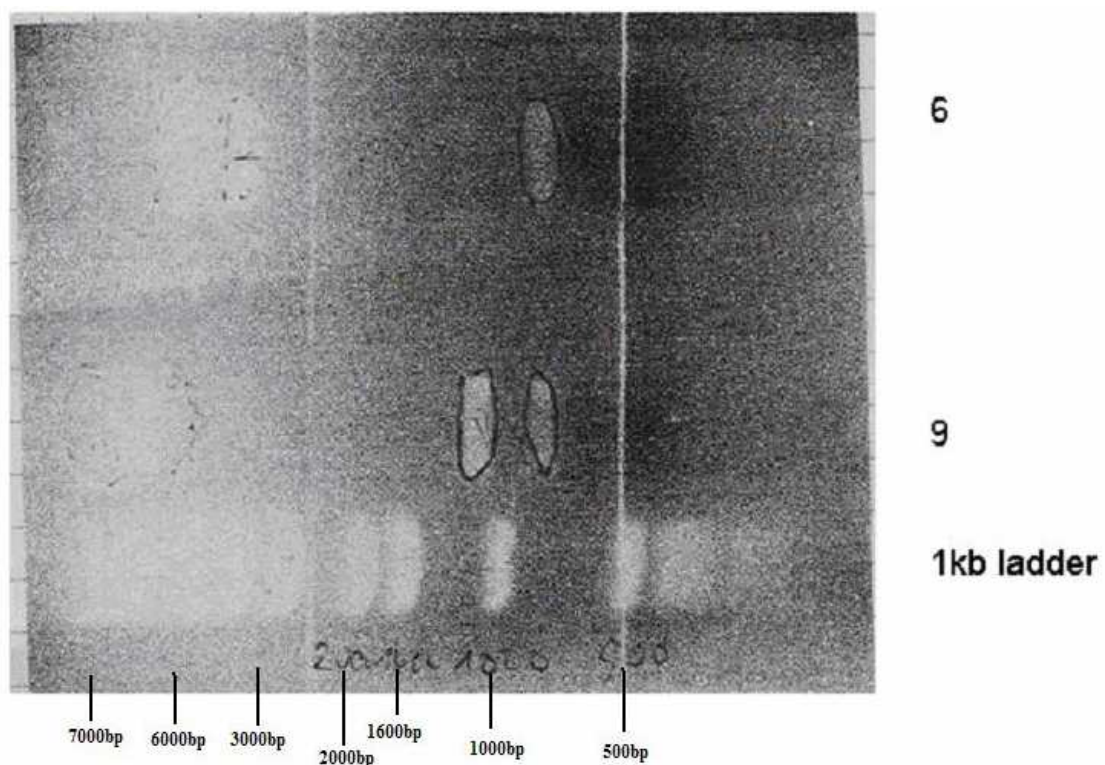


Fig. 19: Restriction digestion of minipreps 6 and 9 with Bgl II.

Based on the restriction scheme in Fig.20 the right orientation would result in three fragments of 860 + 1400 + 7357 bp, the wrong orientation in the fragments 860+3433+6184bp. In miniprep 6 the 1400 bp fragment was clearly missing, but it was present in miniprep 9, indicating the successful subcloning for miniprep 9 (Fig.19).

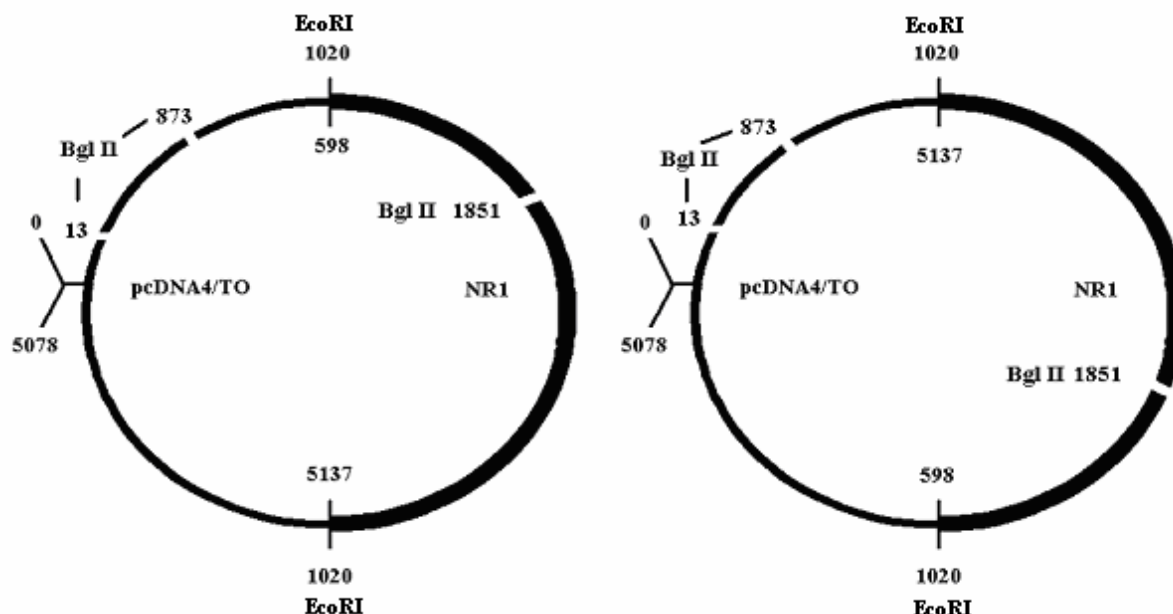


Fig 20: Bgl II cut of NR1/pcDNA4/TO with correct insertion on the left and the opposite insertion on the right. Outer numbers indicate positions of restriction sites within the vector, inner numbers the positions within the insert.

Miniprep 9 was proliferated for further experiments.

2.1.2.2. Transient transfection of NR1 and NR2A subunits

Two million cells were plated into 100-mm diameter cell culture dishes one day before transfection. At the day of transfection, the medium was first changed. Six to seven hours later, 3 μ g of NR1/pCDNA4/TO and 3 μ g hNR2A/pCDNAI in 450 μ l of H₂O were mixed with 50 μ l of 2.5M CaCl₂ and the further transfection procedure was as described in 2.1.1.1.

One day after transfection, induction of the receptor was started by treatment with 1 mg/l tetracycline or vehicle as a control. Cells were additionally treated with 500 μ M memantine or 3 mM Mg²⁺ to block against cytotoxic effects of the NMDA receptor, or left untreated or treated with memantine alone. The cells were harvested for binding two days after transfection.

2.1.2.3 Stable transfection of NR1 and NR2A subunits

For stable transfection I used the cDNA of the subunit NR1 in the expression vector pcDNA4/TO which allowed selection with the antibiotic zeocin. Since I had to use the cDNA of the subunit NR2A in the expression vector pcDNAI without any selection marker, I applied 5 times more NR2A/pcDNAI than NR1/pcDNA4/TO for cotransfection reasoning that this ratio would make it very likely that cells resistant to zeocin would not only express the NR1 but also the NR2A subunit.

Two million cells 293/T-Rex cells were plated into 100-mm diameter cell culture dishes one day before transfection. At the day of transfection, the medium was first changed and six to seven hours later, 1 µg of NR1/pcDNA4/TO and 5 µg hNR2A/pcDNAI in 450 µl of H₂O were mixed with 50 µl of 2.5M CaCl₂ and the further transfection procedure was as described in 2.1.1.1. One day after transfection, some plates were split 1:8, other plates were split 1:4 to reach the right density of cell clone selection. Two days after transfection selecting antibiotics were added, zeocin at 0.3 g/l and blasticidin at 5mg/l. After 8 days, medium was changed and new blasticidin and zeocin were added. Five days later single clones were identified by putting the cell culture plates on a black paper. The clones were sucked off with Gilson pipette tips and transferred into 48 well plates pre-filled with 0.5 ml medium per well (+selecting antibiotics). Six days later each of the cell clones was split after trypsinisation into one well of a 24-well plate and one well of a 48-well plate with respective labelling. On the next day tetracycline was added (0.1mg/l) for induction of the NMDA receptor in the 48-well plate. Cell clones dying in the 48-well plate (assumably due to functional NMDA receptor expression) were further grown up from the corresponding 24-well plate by consecutive splitting of confluent cell layers into 6 well plates and finally 100-mm plates. Cells induced by tetracycline and protected against cytotoxic effects by 200 µM memantine were harvested for radioligand binding. Uninduced cells and cells induced by tetracycline with and without memantine were visualized by phase contrast microscopy using a CCD camera.

2.2. Patch-clamp experiments

Thirty to seventy thousand cells were seeded into poly-lysine coated 35 mm tissue culture dishes. Cells with inducible transporter were treated with tetracycline at a final concentration of 0,1mg/l in the medium immediately at seeding (in case of NAT) or on the next day (in case of DAT). Two to three days after seeding, the cells were washed twice with bath solution and finally incubated in 2 ml of bath solution for 30 min until patch-clamp recordings.

One 35-mm plate was used for about 1-1.5 hours. The bath solution consisted of (mmol/l): 4 Tris-HCl; 6.25 4-(2-hydroxyethyl)-1-piperazineethanesulfonic acid (HEPES); 120 NaCl; 5KCl; 1.2 CaCl₂; 1.2 MgSO₄; 130 NaCl; 34 D-glucose and 0.5 ascorbic acid; pH 7.2. The final osmolarity was 300mOsm/l. Patch pipettes were filled with (mmol/l): 130 KCl; 0.1 CaCl₂; 2 MgCl₂; 1.1 EGTA; 9 HEPES; 0.65 TRIS; pH 7.2, with an osmolarity of 270 mOsm/l. The solutions were sterilized by filtration through a 0.2µm filter and stored for up to two weeks in the refrigerator.

2.2.1. Pipette Puller

Patch electrodes were pulled from borosilicate glass capillaries (GB150F-8P, Science Products, Hofhem, Germany) with a programmable Brown-Flaming micropipette puller (P-97; Sutter Instruments Co., USA). The ultimate size and shape of a micropipette is determined by the parameter values that are programmed by the user. A program consists of one or more cycles which, when executed in sequence, will pull the capillary glass inserted in the instrument giving rise to two pipettes. A program can be up to 8 cycles in length and consists of the arbitrary units velocity, time and heat. Heat controls the level of electrical current supplied to the filament. The velocity value determines the point at which the heat is turned off and reflects the speed at which the two carrier bars are moving during the weak pull. Time controls the length of time the cooling air is active. To assess the heat value a ramp test, which is a heating point detection, must be started.

After the first melting point is determined the glass capillary is adjusted in a position where the glass has not yet been melted. Then the ramp test is started again. This procedure is done three times in order to obtain three values from which the median is calculated. The heat setting is recommended to be the ramp test value plus 15 units. In my programs the velocity was in a range from 23 to 30. The time was always constant at 150 and heat was determined as described before. In Fig. 21 there is an example of a program with four steps. More than one step creates a shorter taper and thus a lower pipette resistance. There was no fixed size of velocity and heat which always was a little bit of trial and error in order to get pipettes with a bellied form in contrast to lance shaped ones which were not optimal.

Heat	velocity	Time
565	25	150
565	24	150
560	23	150
560	21	150

Fig. 21: Example for a puller-program

For receiving pipettes with a smaller opening the glass was slightly melted under the microscope with a tungsten filament in a process called heat polishing. Patch electrodes were finally heat-polished to a tip resistance of 3-9 M Ω .

2.2.2 Drug application device

Test drugs like amantadine and cocaine were applied with a PTR-2000/DAD-12 drug application device (ALA Scientific Instruments Inc., Westbury, NY), allowing a complete exchange of solutions surrounding the cells under examination within <100ms. During measurements cells were continuously superfused with bathing solution.

The DAD system is needed for a programmed application of substances which are filled in 12 syringes. The liquid column is under constant air pressure. Low voltage digital signals direct power to valves to effect open and closed states. In the open state the air pressure forces the test substance with a certain concentration through a tube which is connected with the manifold, a high tech construct made of 13 capillaries derived from gas chromatography which discharge into one small opening. With the manifold the cells are superfused permanently with buffer and for a fixed time point with buffer containing the drug of interest. The DAD is connected with a PC which allows to be programmed in a way that the valves filled with different test drugs are opened and closed for a certain time period until the program ends. The DAD is also connected with another PC with the software clampex which assures the recordings of previously installed DAD programs.

2.2.3. Voltage clamp mode

Recordings were performed in the whole cell configuration using an Axopatch 200B patch-clamp amplifier and the pClamp data acquisition system (Axon Instruments, Foster City, CA, USA) at room temperature (approx. 25°C).

As the patch clamp recording uses a single electrode to voltage clamp the cell, it allows the researcher to keep the voltage constant while observing changes in current. The voltage clamp configuration is depending on the Ohm's law $U=I \times R$. In the case of a steady voltage you can measure the influx as I which is getting higher if the resistance is getting lower according to $U/R=I$. In the voltage clamp modus ($V=-70\text{mV}$) recordings of experiments with different test drugs and ligands were performed eliciting or inhibiting an inward current.

2.3. Uptake-experiments

Cells were seeded in poly-D-lysine-coated 24-well plates (1.3×10^5 DAT/TO cells/well and 1×10^5 293N17 cells/well) and, 1 day later uptake was performed. The uptake buffer consisted of (mmol/l): 4 Tris-HCl; 6.25 4-(2-hydroxyethyl)-1-piperazineethanesulfonic acid (HEPES); 120 NaCl; 5KCl; 1.2 CaCl_2 ; 1.2 MgSO_4 ; 34 D-glucose and 0.5 Na-ascorbate; pH 7.1.

Solutions in the multi-well plates were quickly removed using a Pasteur pipette connected to vacuum pump with a washing bottle in between and added by a repeating pipette. First, the cell culture medium was sucked off. Cells were washed with 500 μl uptake buffer and incubated in 400 μl buffer. Then 50 μl of a tenfold stock solution of cocaine or amantadine in uptake buffer was added. Uptake was initiated by addition of 3 μM [^3H]-DA and went on for 2.5 min at 25°C on a slide-warmer. Uptake was stopped by sucking off the 500 μl and washing the wells twice with 1 ml of ice-cold uptake buffer. Finally, 400 μl of 1% SDS were added to the cells, heated in a microwave oven for 20sec, and the SDS solution was transferred into 5ml-minivials using a 1ml Gilson pipette. Radioactivity was determined in a liquid scintillation counter after addition of 3ml water-miscible scintillation cocktail. For determination of total activity, 50 μl 3 μM [^3H]-DA was mixed with 400 μl 1% SDS and 3 ml liquid scintillation cocktail.

2.4. Superfusion

Cells were seeded onto poly-D-lysine-coated 5-mm-diameter glass coverslips in 96-well tissue culture plates at a density of 40000 cells per well. One day later DAT or NAT expressing cells were loaded with 6 or 0.5 μM [^3H]1-methyl-4-phenylpyridinium (MPP^+), respectively, in 50 μl uptake buffer at 37°C for 20 min. The coverslips were then transferred into small superfusion chambers and superfused with the same buffer as used for uptake experiments (25°C, 1.0 ml/min). After a wash out period of 45 min to establish a stable efflux of radioactivity, the experiment was started by collecting 4-min fractions into 20-ml tubes using a fraction collector. Three fractions were collected to obtain a baseline value, then superfusion was switched to a buffer containing the various drugs of interest for 3-4 fractions. At the end of the experiment superfusion of 1 % SDS eluted the total radioactivity in the cells on the coverslip. The radioactivity in the superfusates and the SDS-lysates was determined by liquid scintillation counting after addition of 6 (buffer fractions) to 10.5 ml (SDS-fractions) scintillation cocktail. The radioactivity released during a specific 4min fraction was expressed as percentage of the total radioactivity present in the cells at the beginning of each fraction by adding up radioactivity in the respective and all following fractions including the SDS-fraction.

2.5. Radioligand binding on NMDA receptor expressing cells

For harvesting 3x 100 mm plates were put on ice, cell culture medium was sucked off, cells were washed with 10 ml PBS and 5 ml PBS was added to each plate. Then cells were scraped from the first plate in 5 ml PBS and transferred into a 50 ml falcon tube. This was repeated for the remaining plates. Then the three plates were consecutively rinsed with 5 ml PBS and this added up to a total of 20 ml cell suspension which was centrifuged for 10 min at 2400rpm. The pellet was re-suspended in 30 ml of buffer (50mM Tris-acetate, pH 7.0), and centrifuged for ½ hour at 4°C with 17000rpm in a SS34-rotor. The resulting pellet was resuspended in 500 μl buffer and frozen at -80 °C.

For the binding assay, frozen samples were replenished with 10 ml buffer in SS34-tubes, homogenized with a repeating pipette and finally filled up to 35 ml with buffer and centrifuged 30 min at 17000 rpm. Pellet was resuspended in 500 μl buffer with the repeating pipette resulting in the final membrane preparation. Three hundred μl of buffer, 50 μl of 100 μM glutamate/glycine, 50 μl of 50nM [^3H]MK801 and 100 μl membrane preparation were mixed and incubated for 2h at 24°C.

For unspecific binding 50 μ l of a mixture of 100 μ M CGP39653(Ciba Geigy)/10 μ M L701324(Merck Sharp & Dohme) instead of glutamate/glycine was used.

Incubation was stopped by addition of 4 ml of ice-cold buffer and rapid filtration through Whatman GF/B Filters presoaked for 1h in polyethylenimine (0.3% in H₂O), using a 48-place Brandel (Gaithersburg, MD) harvester. Filters were washed twice with 4ml ice-cold buffer and transferred into counting vials. 1.8 ml of scintillation cocktail was added and vials shaken vigorously. Thereafter vials were agitated for 20min. Two samples with 1.8 ml of scintillation cocktail and 50 μ l of 50nM [³H]MK801 were prepared for measurement of total activity. Radioactivity was counted with liquid scintillation counter.

The protein content of the membrane preparation was determined by the Bio-Rad Protein assay based on the method of Bradford. Since the membrane preparation was diluted 1:10 in water, the protein standard (bovine serum albumine, BSA) was dissolved in 5mM Tris-acetate. Five dilutions containing 2, 4, 8 , 12 and 16 μ g BSA/50 μ l were prepared. The assay was performed in duplicates by mixing 750 μ l H₂O with either 50 μ l 5mM Tris-acetate for autozero or 50 μ l standard solution or 50 μ l 1:10 diluted membrane preparation and 200 μ l of dye reagent concentrate in photometer vials and incubation for 20 min at room temperature. Absorbance of samples was measured at 595nm.

2.6. Cell viability assay

Cell viability was determined in 96 well plates. Five thousand cells were seeded in 200 μ l medium per well. One day later the NAT or the NR1/2A receptor was induced by tetracycline at a final concentration of 0.1mg/l by adding 2 μ l of a 100x stock to 200 μ l medium and the cells were exposed to various drugs (desipramine, amantadine, ketamine ..) by adding 4 μ l of a 50x stock to 200 μ l medium or H₂O as vehicle. Toxicity in NAT expressing cells was induced by adding 2 μ l of a 100x stock to 200 μ l medium to obtain a final concentration of 1 μ M MPP⁺. Two μ l H₂O was added as vehicle. The application scheme for the various drugs is shown in Fig.22

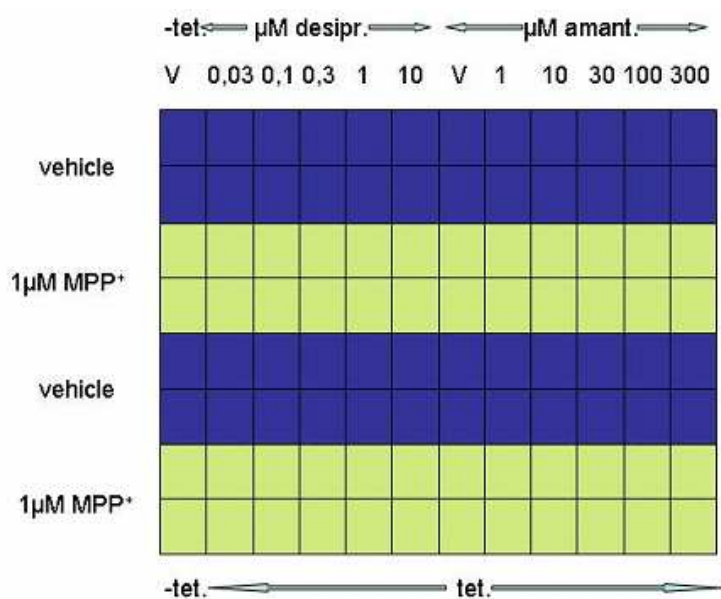


Fig. 22: Application scheme of substances for hNAT expressing cells in 96-well plates. Cells in the first column of wells on the left were not induced (-tet), all other wells were treated with 0,1mg/l tetracycline (tet.). Column of wells were treated with vehicle (V) or increasing concentrations of desipramine or amantadine as indicated. Four rows of wells (yellow) were treated with 1 µM MPP⁺ as toxic agent or stayed untreated (vehicle, blue).

Toxicity in NR1/2A cells was observed one day after receptor induction presumably due to glutamate in the culture medium. The application scheme for the various drugs is shown in Fig.23

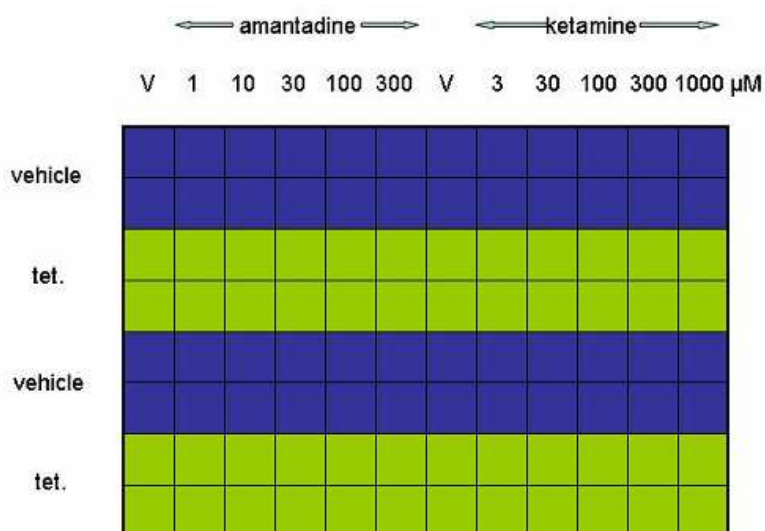


Fig. 23: Application scheme of substances for NR1/2A expressing cells in 96-well plates. Column of wells were treated with vehicle (V) or increasing concentrations of amantadine or ketamine as indicated. Four rows of wells were treated with tetracycline for induction of toxicity mediated by expression of the NMDA receptor (tet., green) or stayed untreated (vehicle, blue).

Three days after administration of drugs to NAT-cells and one day after administration of drugs to NR1/2A-cells the number of living cells was estimated by measuring acid phosphatase activity according to Yang and coworkers (1996). First, cells were washed with 200 μ l PBS. Then cells were incubated with 100 μ l of NPP buffer (0.8232 mg p-nitrophenylphosphate + 9.9 ml H₂O + 1.1ml 1 M sodiumacetate, pH 5.4, in 1 % triton X-100). Forty eight wells were handled in a row. Incubation was at 37°C for two hours. The reaction was stopped by addition of 10 μ l of a 1M NaOH solution. Absorbance was measured at 405 nm in the microplate reader.

3. Results

3.1. Uptake experiments on NAT or DAT expressing cells

Several publications reported effects of amantadine on monoamine neurotransmission in rodents (see chapter 1.3.). Therefore, it seemed to be interesting to investigate the effect of amantadine for the first time on the human NAT and DAT. First, the uptake of [3 H]DA was measured in NAT and DAT expressing cells in presence of increasing concentrations of cocaine and amantadine (Fig. 24).

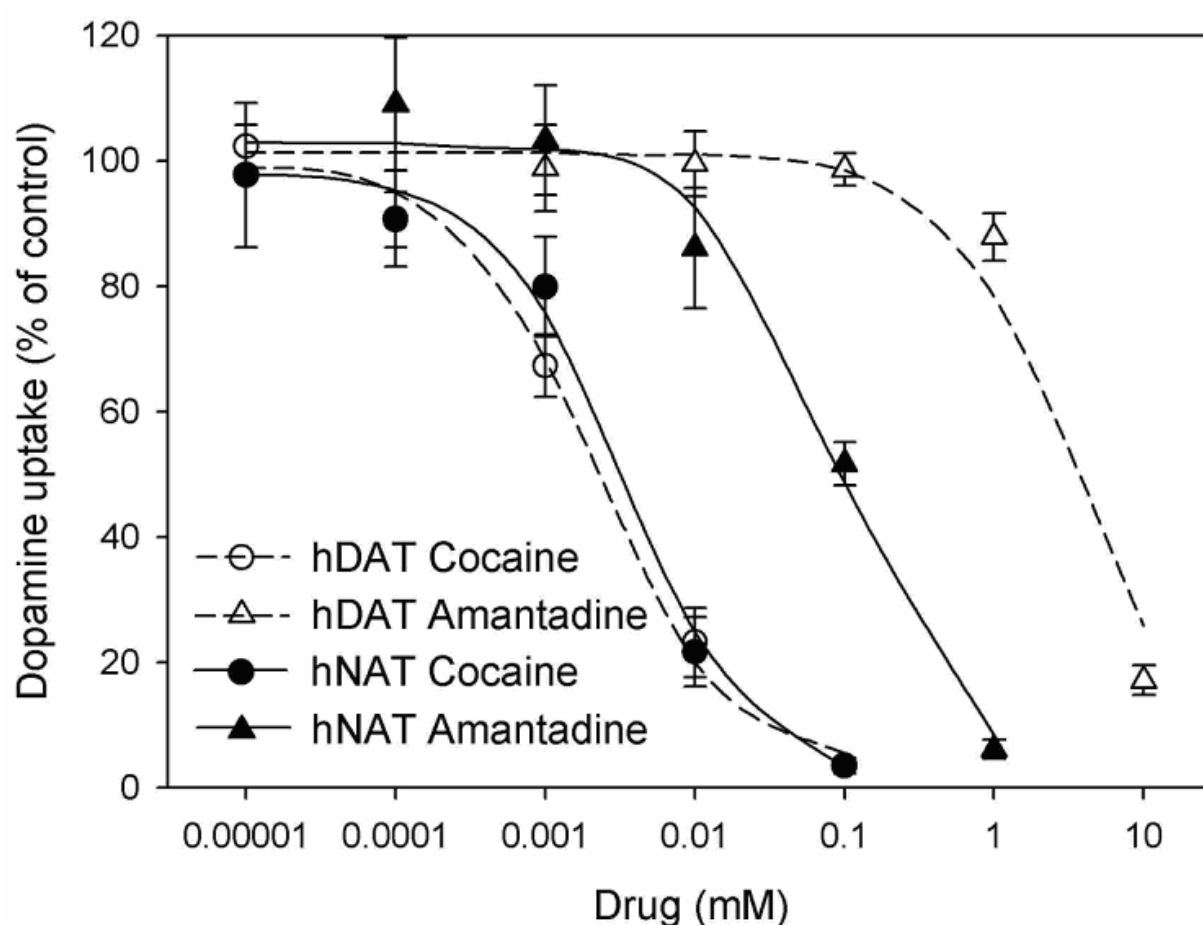


Fig. 24: Uptake of DA in HEK-cells expressing the human DAT (open symbols) and the human NAT (closed symbols) under increasing concentrations of cocaine and amantadine as indicated. Symbols represent means \pm standard error of n independent experiments, each in duplicates. $n=10$ for amantadine in DAT, $n=6$ for cocaine in DAT, $n=8$ for amantadine in NAT, $n=4$ for cocaine in NAT. The data of each experiment were fitted by nonlinear regression.

Amantadine was able to block the uptake by the NAT or DAT in a concentration-dependent manner and had a 15 fold higher potency for blocking the NAT than the DAT. Cocaine, as positive control, was nearly equipotent at the DAT and NAT and about 15 fold more potent than amantadine at the NAT.

3.2. Release experiments on NAT expressing cells

The effect of amantadine in uptake experiments could be due to pure uptake inhibition similar to the action of cocaine, or due to a releasing action. Therefore, the effect of amantadine was studied in superfusion experiments and its effect was compared to amphetamine as a positive control (Fig.25).

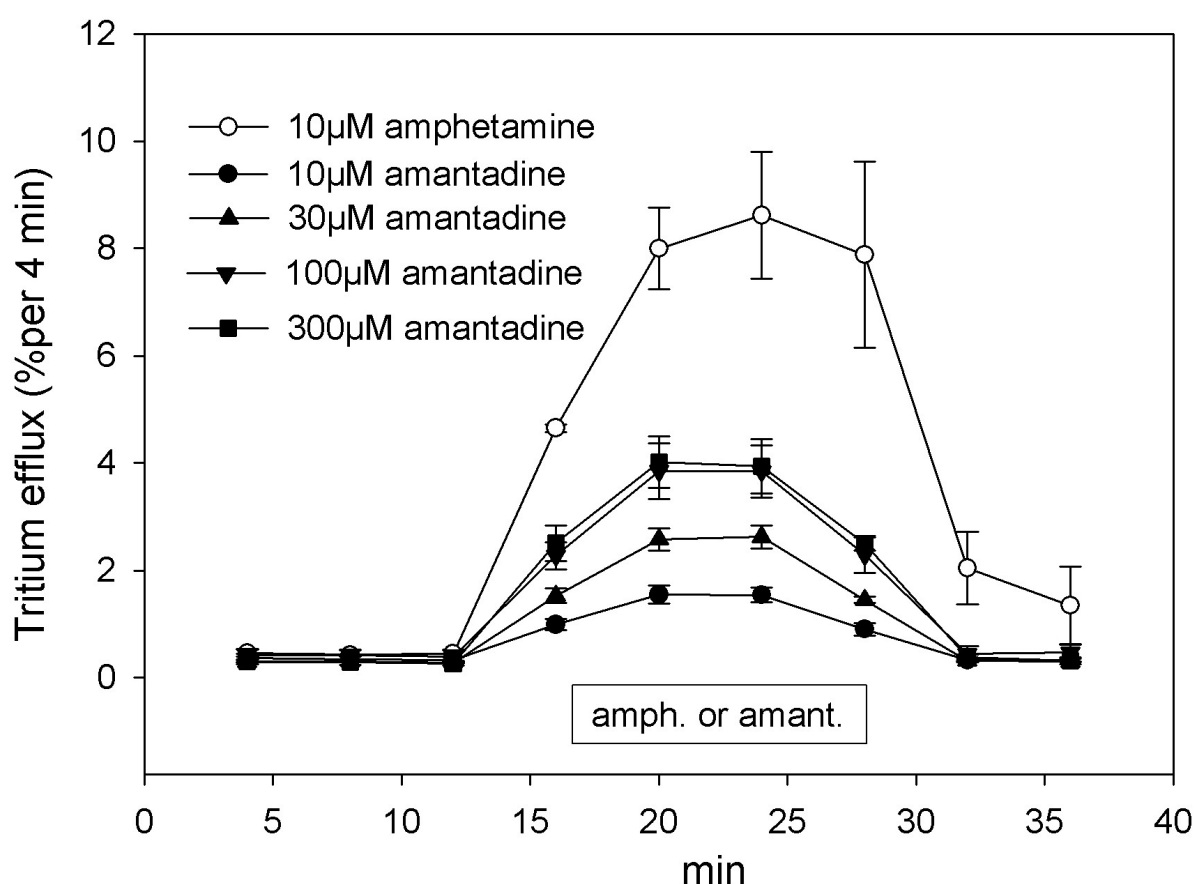


Fig. 25: Superfusion of HEK293 cells stably expressing the human NAT grown on 5-mm-diameter coverslips and preloaded with [^3H]MPP $^+$. Effects of amphetamine and amantadine induced release of [^3H]MPP $^+$ at the concentrations indicated. Bar indicates fractions after exposure to amphetamine or amantadine. Symbols represent means \pm standard error of three independent experiments.

In these superfusion experiments one can clearly see that amantadine acted as a releasing drug, however its intrinsic activity was about half of that of amphetamine as the maximally induced tritium efflux was 4% per 4 min fraction as compared to 9% per 4 min fraction induced by 10 μ M amphetamine, a concentration of amphetamine which is nearly maximally active as reported previously (Sitte et al., 1998).

The releasing effect of 100 μ M amantadine was completely suppressed by the presence of 10 μ M mazindol (Fig.26)

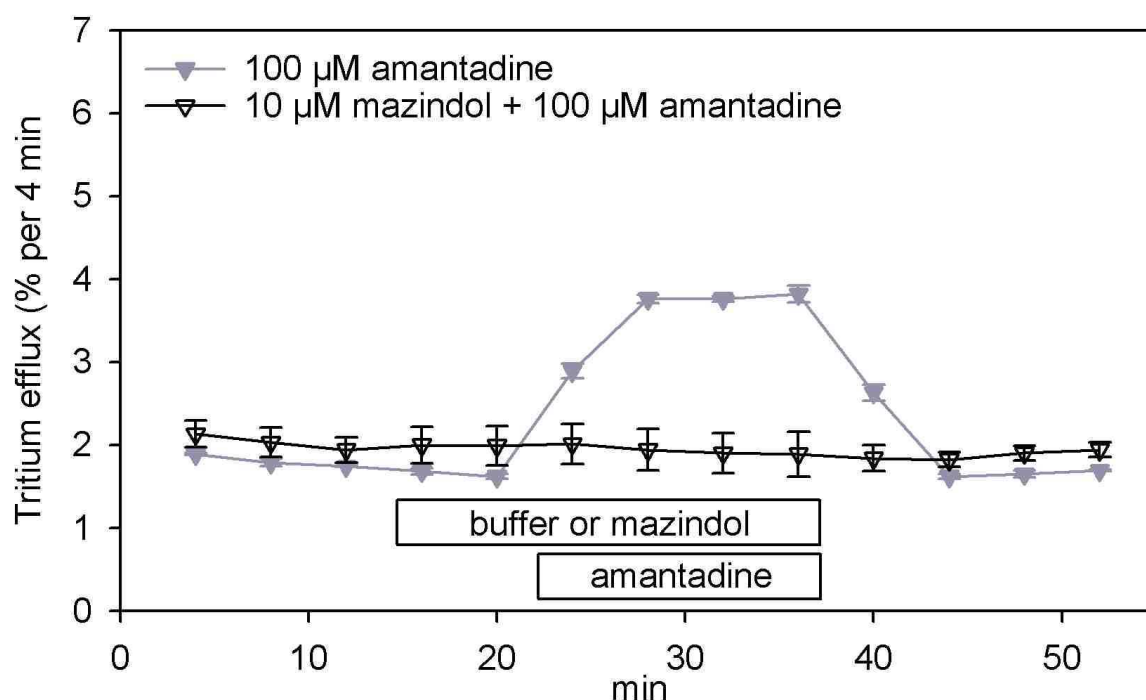


Fig. 26: Superfusion of HEK293 cells stably expressing the human NAT grown on 5-mm-diameter coverslips and preloaded with [3 H]MPP $^+$. Bars indicate fractions after exposure to mazindol or amantadine. Symbols represent means \pm standard error of 3 independent experiments.

This concentration of mazindol also blocked the releasing effect of 10 μ M amphetamine completely (Fig. 27).

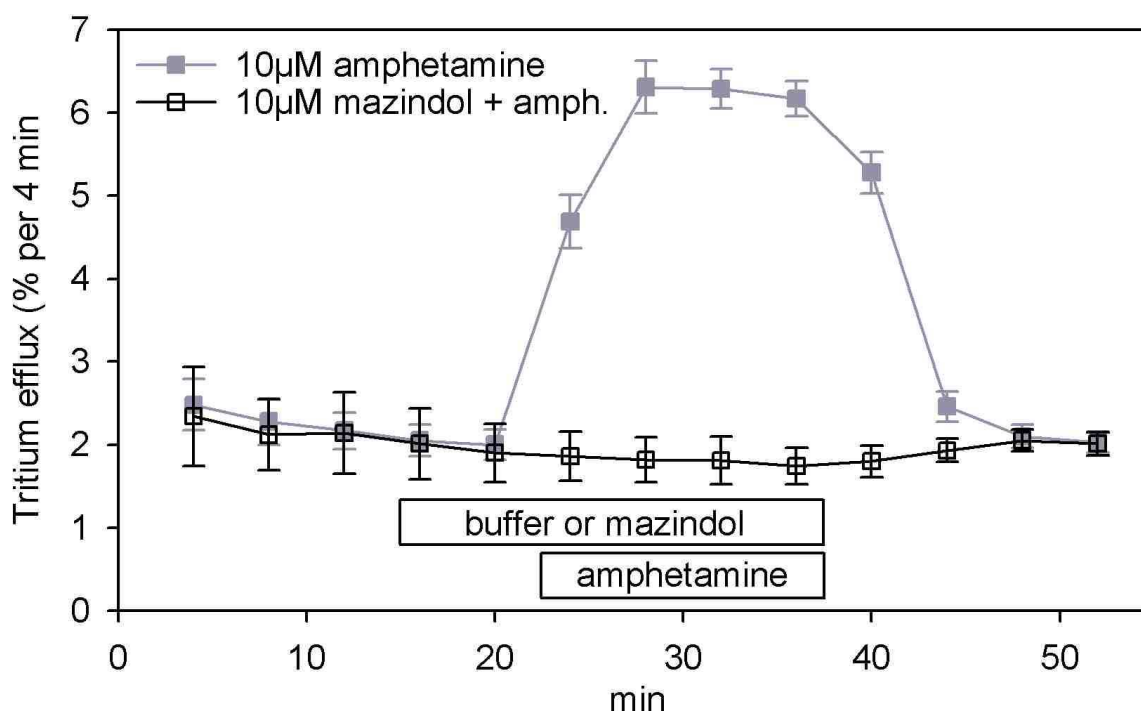


Fig. 27: Superfusion of HEK293 cells stably expressing the human NAT grown on 5-mm-diameter coverslips and preloaded with [^3H]MPP $^+$. Bars indicate fractions after exposure to mazindol or amphetamine. Symbols represent means \pm standard error of 3 independent experiments.

3.3. Patch-clamp experiments

3.3.1. Patch-clamp experiments on NAT expressing cells

The type of interaction of a substance with plasmalemmal neurotransmitter transporters can be investigated by the patch-clamp technique. Therefore, I voltage-clamped HEK293 cells expressing the human NAT in the whole-cell configuration. In a first series of experiments the effects of NA and amantadine, each administered alone, were investigated. (Fig. 28).

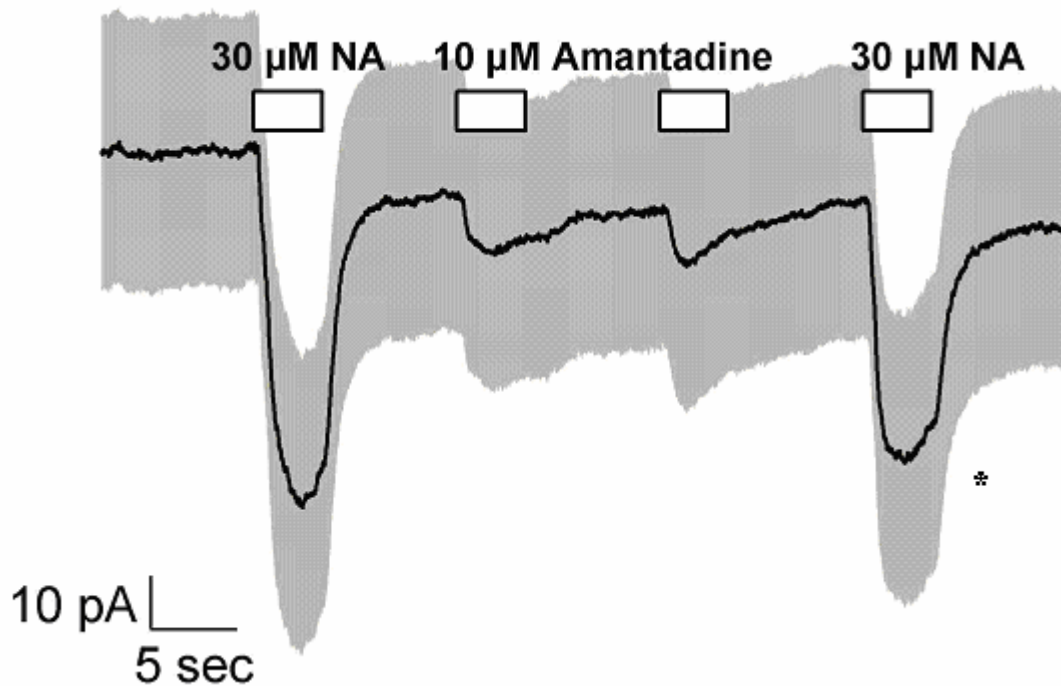


Fig. 28: Effects of amantadine on whole-cell patch-clamp recordings of HEK293 cells stably and inducibly expressing the human NAT. The cells were voltage-clamped at a holding potential of -80mV and superfused at the times marked by the bars for 4 s with noradrenaline and amantadine at the concentrations indicated. Shown are mean values of current traces \pm SEM (grey area) of 19 cells. * $p < 0,02$ versus first NA-induced inward current by paired Student's t-test..

After a forerun of buffer lasting for 8 seconds 30μM NA was superfused for 4 seconds causing an inward current of about 60pA. Repeated superfusion of amantadine for 4 seconds with buffer for 8 seconds in between, led to an inward current of about 10 pA. A second superfusion with 30μM NA also triggered an inward current which was significantly smaller (45 pA) than the first one which might be due to a phenomenon of desensitization in these experiments.

In another program of superfusion, the effects of NA and amantadine, which were administered alone and together, were investigated (Fig. 29).

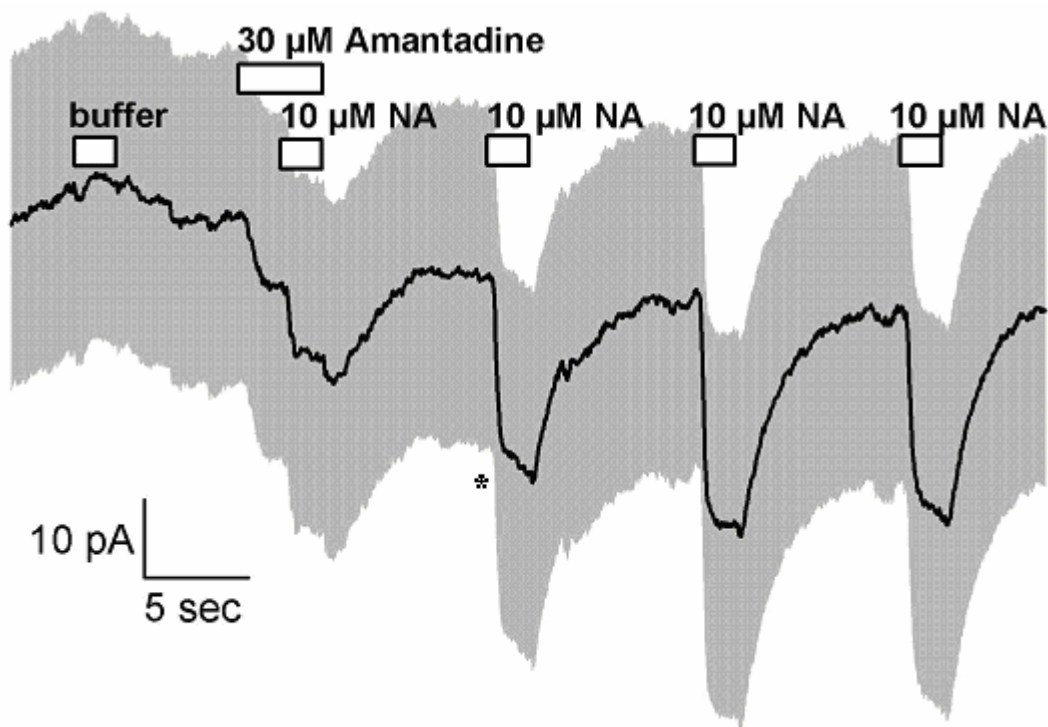


Fig. 29: Effects of amantadine on whole-cell patch-clamp recordings of HEK293 cells stably and inducibly expressing the human NAT. The cells were voltage-clamped at a holding potential of -80mV and superfused at the times marked by the bars for 2 s with 30 μ M amantadine or 10 μ M NA. Shown are mean values of current traces \pm SEM (grey area) of 15 cells. * $p < 0,0005$ versus NA-induced inward current in the presence of 30 μ M amantadine.

A 2-second switch of superfusion from one buffer-containing syringe to another buffer-containing syringe did not induce any change of current. Superfusion with 30 μ M amantadine induced an inward current of about 10 pA, and 10 μ M NA in the continued presence of amantadine caused an additional inward current of about 10 pA. The following 3 repetitions of 2-second superfusions with 10 μ M NA alone led to an influx of about 25pA without signs of desensitization. These experiments demonstrate an attenuating effect of amantadine on NA-induced inward currents.

If currents induced by NA and modified by amantadine are related to the NAT it should be affected by the NA uptake blocker cocaine. Therefore, I investigated the effect of cocaine in the next series of experiments (Fig.30).

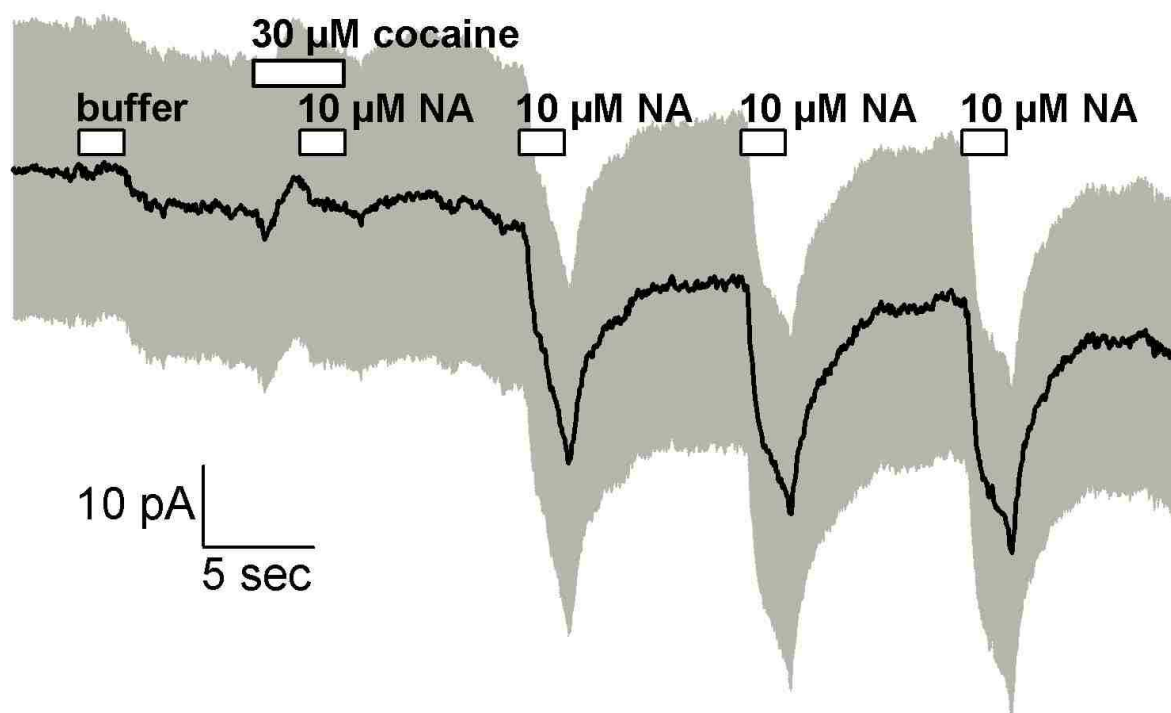


Fig. 30: Effects of cocaine on whole-cell patch-clamp recordings of HEK293 cells stably and inducibly expressing the human NAT. The cells were voltage-clamped at a holding potential of -80mV and superfused at the times marked by the bars for 2 s with 30 μ M cocaine and/or 10 μ M noradrenaline. Shown are mean values of current traces \pm SEM (grey area) of 14 cells.

A forerun of buffer for 8 seconds was followed by a 2-second superfusion of 30 μ M cocaine and a subsequent application of 10 μ M NA in the continued presence of 30 μ M cocaine. Cocaine induced a small outward current of about 5-10pA which can be explained by blockade of a leak current in NAT-expressing cells. In the presence of cocaine NA was without effect, however the blocking action of cocaine could be washed out since after 8 seconds of buffer three repeated applications of 10 μ M NA for 2seconds each elicited inward currents of about 30 pA.

3.3.2. Patch-clamp experiments on DAT expressing cells

First the effect of amantadine was compared with that of DA (Fig.31).

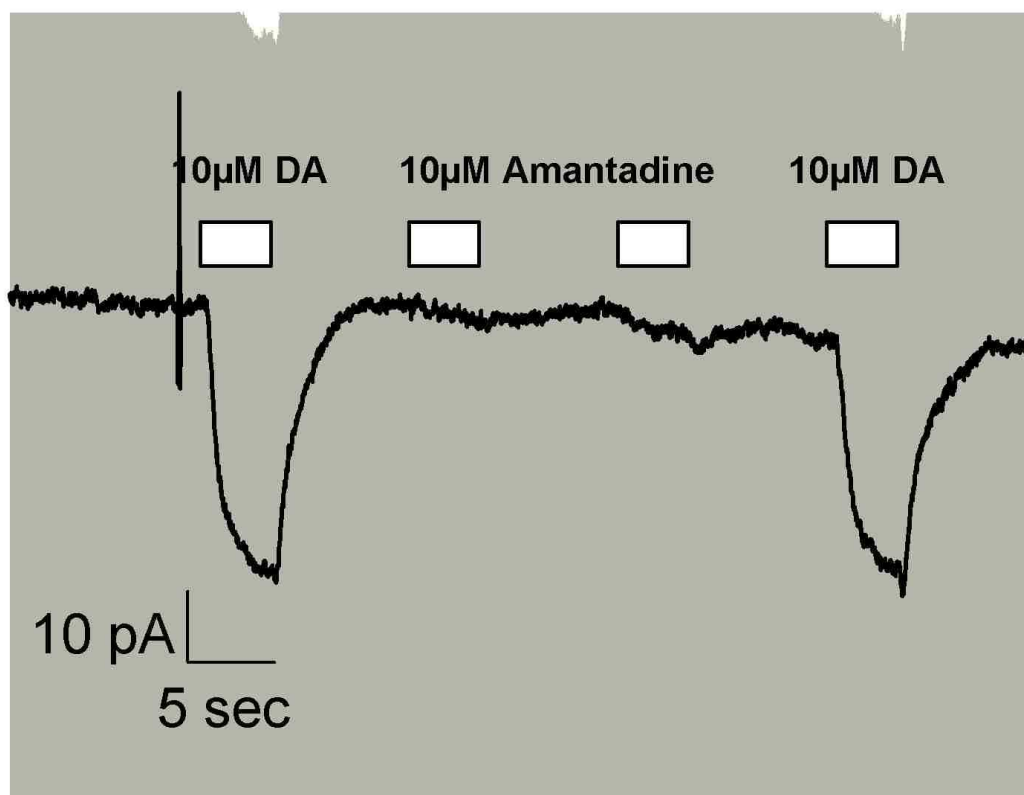


Fig. 31: Effects of Am on whole-cell patch-clamp recordings of HEK293 cells stably and inducibly expressing the DAT. The cells were voltage-clamped first at a holding potential of -80mV and superfused at the times marked by the bars for 4 s with DA or Am at the concentrations indicated. Shown are mean values of current traces \pm SEM (grey area) of 7 cells.

After an 8-second forerun of buffer, superfusion of 10μM DA for 4 seconds elicited an influx of about 40 pA. After a washout with buffer for 8 seconds repeated administration of 10μM amantadine for 4 seconds had no significant effect and application of 10μM DA for 4 seconds at the end of the superfusion program led again to an inward current of approx. 40 pA.

Since amantadine had no effect on the DAT on its own, the question was whether it modified the effect of a transporter substrate on the DAT. Therefore, I designed a superfusion program,

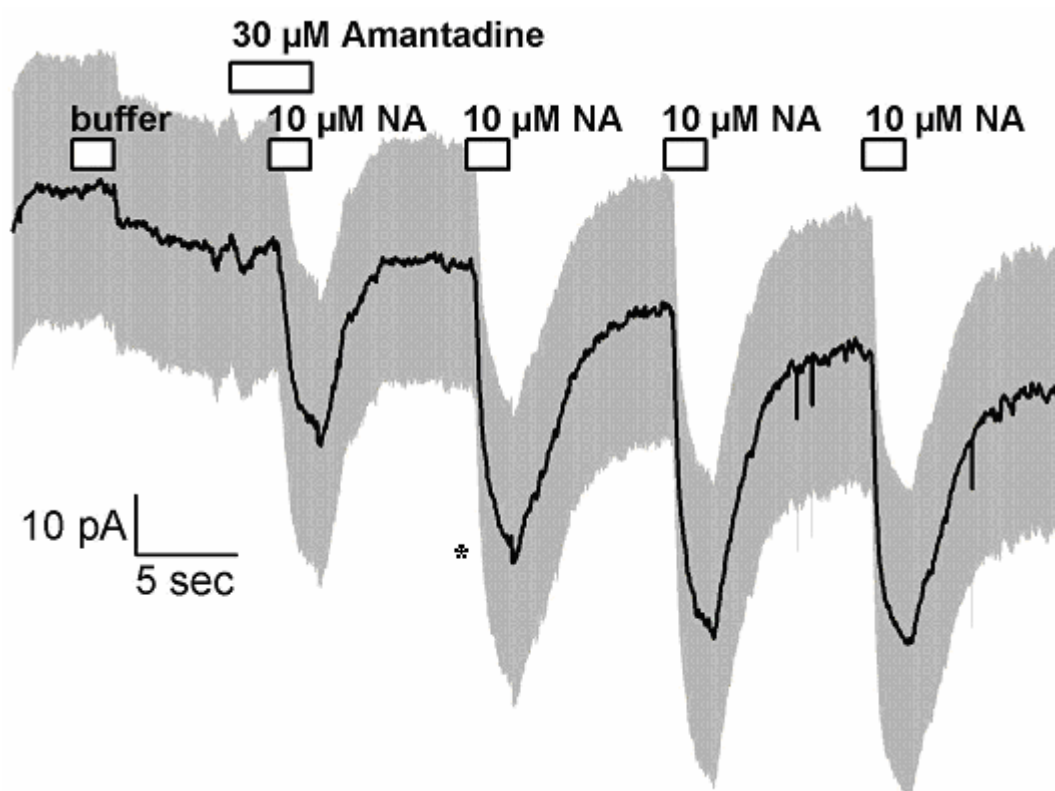


Fig. 32: Effects of Am on whole-cell patch-clamp recordings of HEK293 cells stably and inducibly expressing the DAT. The cells were voltage-clamped first at a holding potential of -80mV and superfused at the times marked by the bars for 2 s with Am or Am in presence of NA or NA alone at the concentrations indicated. Shown are mean values of current traces \pm SEM (grey area) of 10 cells. $p > 0.05$ versus first inward current of NA in presence of Am.

where I could assess the effect of amantadine and NA alone and a combination of both (Fig. 32). After a forerun of buffer for 8 seconds superfusion with 30 μ M amantadine for 2 seconds induced a minor, transient inward current and subsequent superfusion of 10 μ M NA in the continued presence of 30 μ M amantadine elicited an inward current of about 30 pA. After buffer washout three 2-second applications of NA (alternating with 8-second applications of buffer) led to an inward current of about 40 pA which was significantly higher than the effect of the combination of NA with amantadine. This hints to a small blocking effect of amantadine on the DAT.

This DAT blockade was much weaker than that by the prototypic DAT blocker cocaine. In my last patch-clamp experiment the effect of cocaine alone and its effect on the DAT substrate NA was investigated (Fig.33).

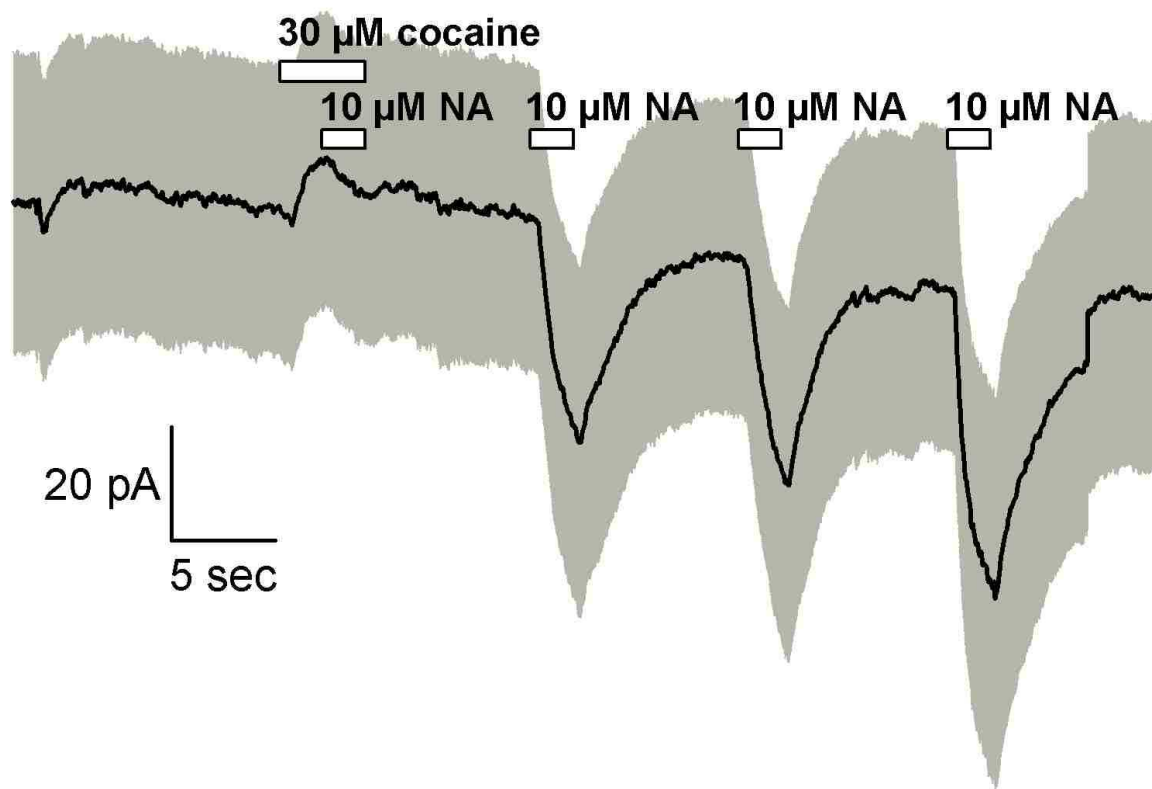


Fig. 33: Effects of cocaine on whole-cell patch-clamp recordings of HEK293 cells stably and inducibly expressing the DAT. The cells were voltage-clamped first at a holding potential of -80mV and superfused at the times marked by the bars for 2 s with cocaine or cocaine in presence of NA or NA alone at the concentrations indicated. Shown are mean values of current traces \pm SEM (grey area) of 12 cells.

A forerun of buffer for 8 seconds was followed by superfusion of 30 μ M cocaine for 2 seconds, a subsequent combination of 30 μ M cocaine with 10 μ M NA for another 2 seconds and, after a 8-second washout with buffer, three repeated applications of 10 μ M NA, 2 seconds each, with 8 seconds of buffer in between. Cocaine elicited as small outward current of less than 10 pA similar to its effect at NAT expressing cells. The combination of cocaine and NA was essentially baseline and after a washout with buffer for 8 seconds the repeated NA applications led to inward currents of about 30pA revealing a total recovery of the NAT function after cocaine is washed away.

3.4. Characterization of cells expressing the human NR1/2A receptor

3.4.1. Radioligand binding after transient transfection

First I cotransfected equal amounts of the subunits NR1- and NR2A-cDNA into 293/T-Rex cells and assessed the formation of functional receptors by binding of the radioligand [³H]MK-801 to membranes prepared from these cells.

Specific binding in fmol/tube	
uninduced	0.696
receptor induced	16.94
hippocampal membranes	39.16

Table 1: Binding results of transient transfection.

Due to variable amounts of protein per tube (2.5 µg in uninduced cells, 58.8 µg in induced cells, and 36.9 µg in hippocampal membranes) specific binding per mg protein was not higher in induced than in uninduced cells after transient transfection.

3.4.2. Cytotoxicity after stable transfection

Cell clones surviving the selecting antibiotic were grown up and on each clone the effect of induction by tetracycline on viability was determined. Effects of receptor-induction by tetracycline and the protective effect of the NMDA-receptor antagonist memantine was visualized in selected clones seeded in a 24- and a 12-well plate by phase contrast microscopy (Fig.34 and Fig.35).

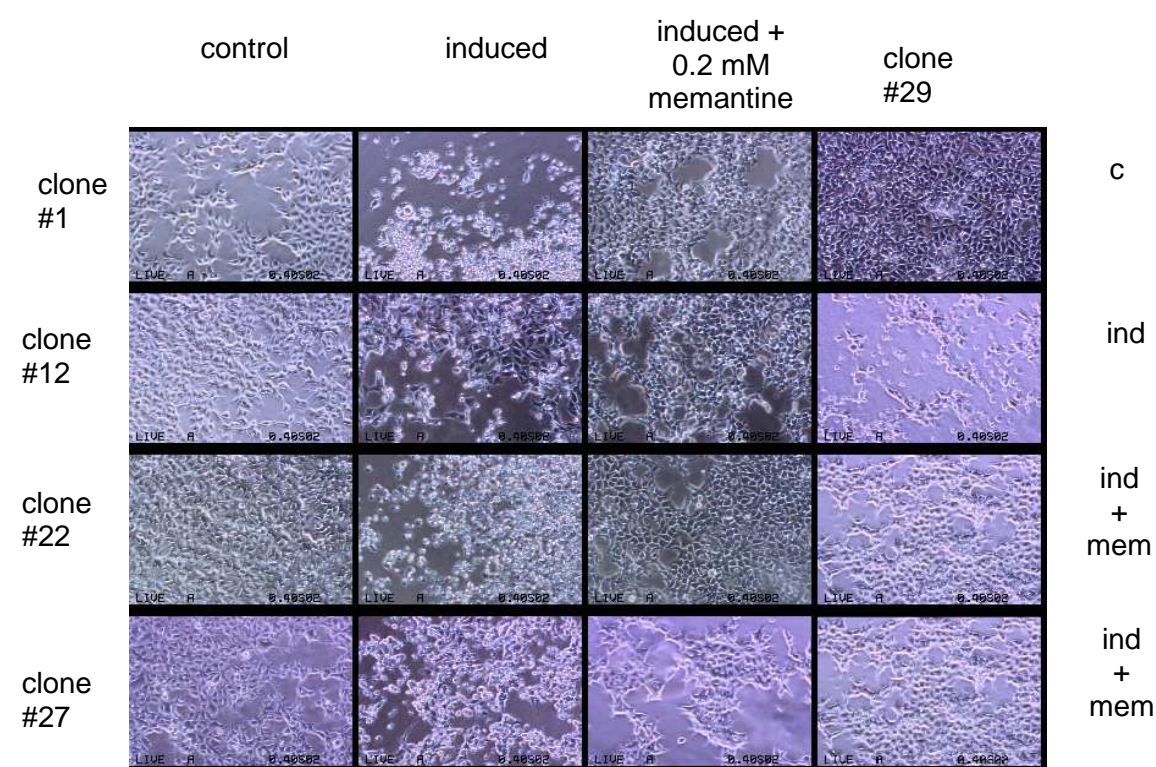


Fig. 34: Phase contrast microscopy of different clones in a 24-well plate after induction with tetracycline in the absence or presence of 200 μ M memantine as well as without induction as a control.

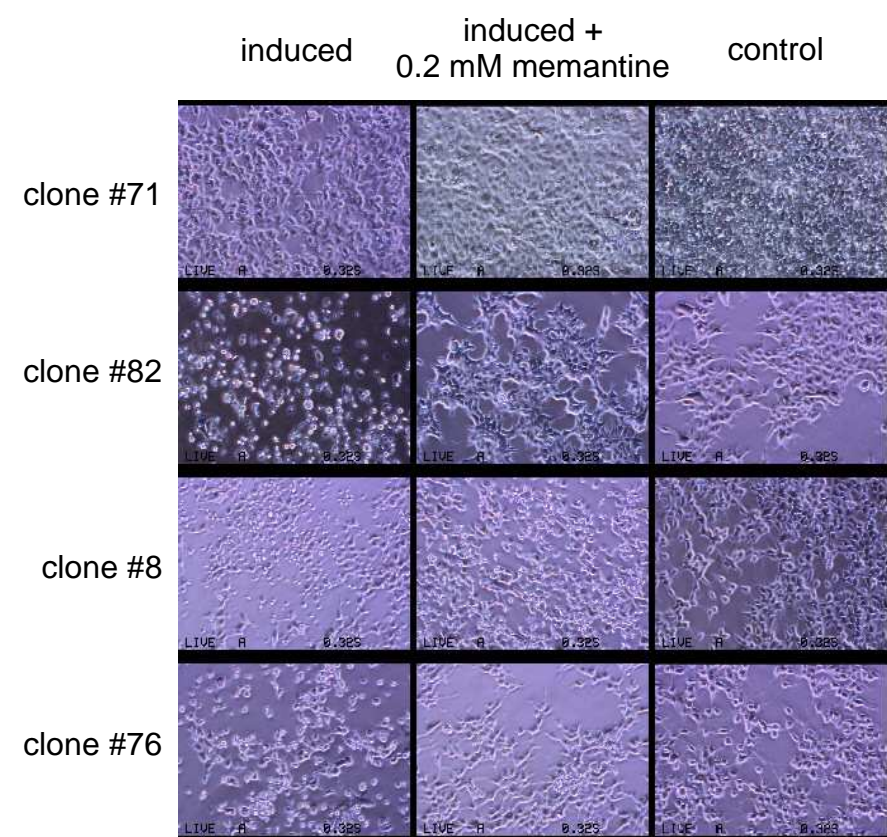


Fig.35: Phase contrast microscopy of different clones in a 12-well plate after induction with tetracycline in the absence or presence of 200 μ M memantine as well as without induction as a control.

Induction of the receptor by tetracycline induced cell death with round, partly floating cells loosing their processes and connections to other cells (Fig. 34 and 35). The presence of 200 μ M memantine provided protection against NMDA receptor mediated autotoxicity and the cells resembled the control cells not induced by tetracycline.

3.4.3. Radioligand binding after stable transfection

Cell clones showing cell death induced by tetracycline were induced in the presence of cytoprotective memantine and harvested for radioligand binding. Cell membranes prepared from human post mortem brain (fronto-parietal cortex) were used as a positive control. The results for the different clones are summarized from two binding experiments in Table 2.

Protein amounts per tube	
clone 1	117.2 μ g
clone 8	4.8 μ g
clone 12	24 μ g
clone 22	116 μ g
clone 27	84 μ g
clone 29	24.4 μ g
clone 71	77.6 μ g
clone 76	70 μ g
clone 82	84 μ g
clone 83	96 μ g
frontoparietal cortex (+control)	138 μ g

Specific binding (pmol/mg protein)	
clone 1	0,009
clone 8	1,61
Clone12	no specific binding
clone 22	0,017
clone 27	0,076
clone 29	0,275
clone 71	0,003
clone 76	0,009
clone 82	0,017
clone 83	0,031
frontoparietal cortex (+control)	0,629

Table 2: Protein amounts and specific binding in different cell clones with inducible expression of the NR1/2A receptor and human cortical membranes as a positive control.

Specific binding varied considerably between cell clones and was much lower than in human cortex, except for clone 29. The result for clone 8 is not reliable due to the small amount of protein.

3.5. Toxicity assays on NAT or NR1/2A-receptor expressing cells

In order to determine the potency of amantadine on the NAT and the NR1/2A-receptor under in vivo conditions, I used a cytotoxicity model where blockade of the NAT or the NR1/2A-receptor produced a concentration-dependent cytoprotective effect.

3.5.1. MPP⁺-induced cytotoxicity in NAT expressing cells

NAT expressing cells were treated with 1 μ M MPP⁺ which enters the cells through the NAT as a gate and decreases cell viability as described previously (Pifl et al., 1996). Treatment of the cells with drugs blocking the NAT increased cell viability in a concentration-dependent manner. The unselective DA and NA uptake blocker mazindol was tested in the range of 0.03 and 10 μ M (Fig.36).

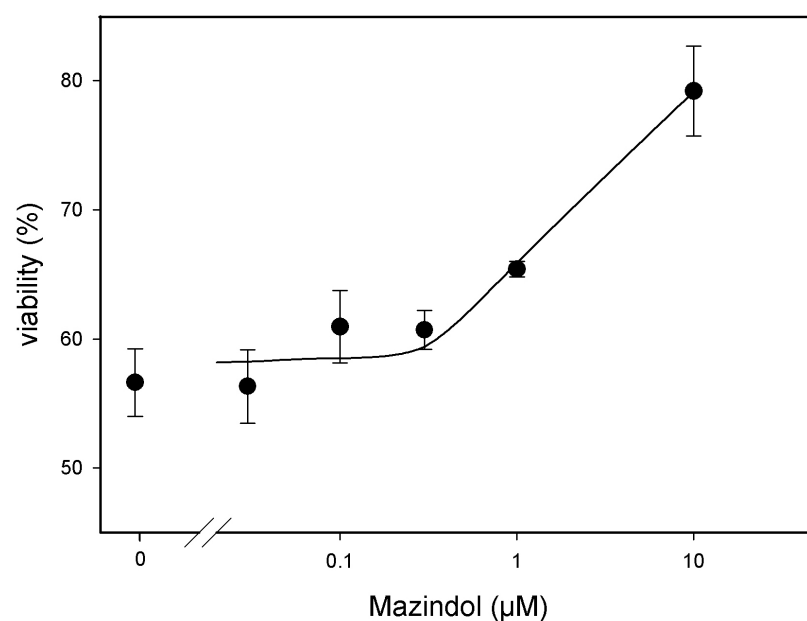


Fig. 36: Effect of mazindol on MPP⁺-induced toxicity in NAT expressing cells. Cells expressing the NAT under the control of the T-RexTM were seeded in 96-well plates and one day later the NAT was induced by treatment with tetracycline, cells were treated with mazindol at the concentrations indicated and toxicity was elicited by 1 µM MPP⁺. Cell viability was determined by measuring acid phosphatase activity 3 days later. Activity was measured in quadruplicates and expressed as percentage of that of vehicle-treated cells. Symbols represent mean values \pm SEM of 2 separate experiments.

At 1 µM there was a weak, at 10 µM mazindol a clear protection against MPP⁺.

In another series of experiments the selective NAT blocker desipramine was tested in the same range of 0.03 to 10 µM (Fig.37). In these experiments, MPP⁺ had a stronger cytotoxic effect decreasing cell viability to 40 % of that of vehicle treated cells.

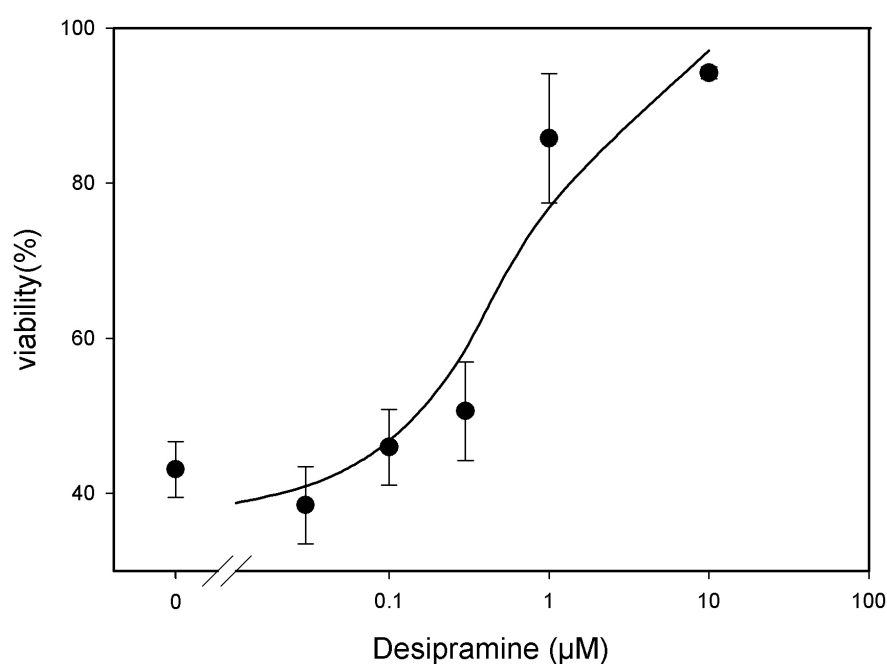


Fig. 37: Effect of desipramine on MPP⁺-induced toxicity in NAT expressing cells. Cells expressing the NAT under the control of the T-RexTM were seeded in 96-well plates and one day later the NAT was induced by treatment with tetracycline and desipramine was added at the concentrations indicated and induction of toxicity by 1 μ M MPP⁺. Cell viability was determined by measuring acid phosphatase activity 3 days later. Activity was measured in quadruplicates and expressed as percentage of that of vehicle-treated cells. Symbols represent mean values \pm SEM of 5 separate experiments.

Desipramine increased cell viability in a concentration-dependent manner with weak effects at 0.1 and 0.3 μ M and nearly restored cell viability at 10 μ M.

I tested the ability of amantadine to protect NAT expressing cells against MPP⁺ cytotoxicity in the concentration range of 3 to 300 μ M (Fig.38).

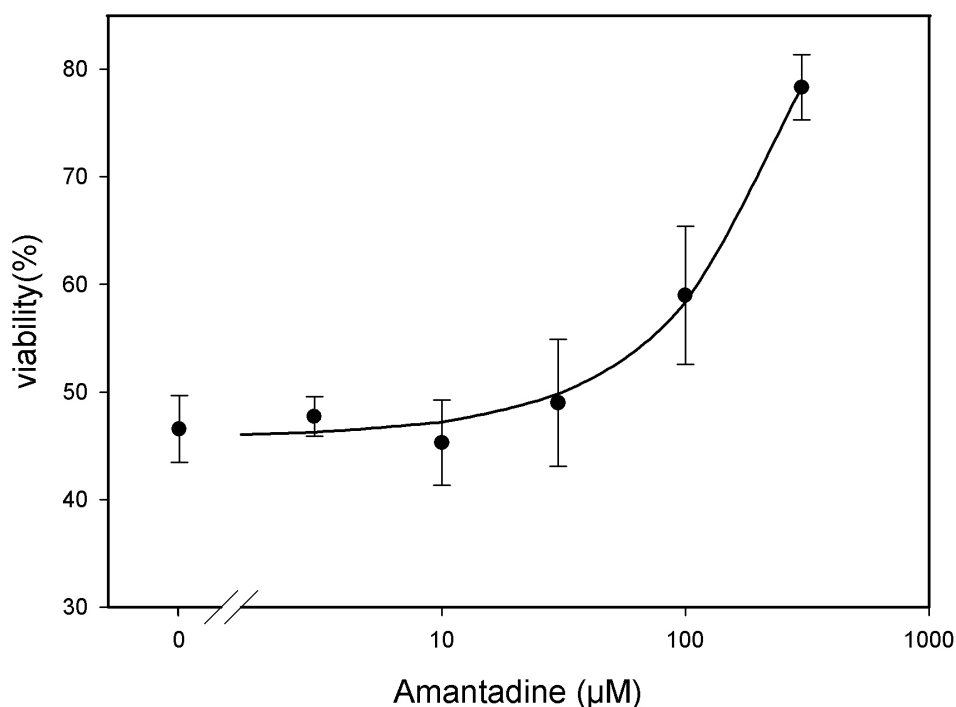


Fig. 38: Effect of amantadine on MPP⁺-induced toxicity in NAT expressing cells. Cells expressing the NAT under the control of the T-RexTM were seeded in 96-well plates and one day later the NAT was induced by treatment with tetracycline, amantadine was added at the concentrations indicated and toxicity was elicited by 1 μ M MPP⁺. Cell viability was determined by measuring acid phosphatase activity 3 days later. Activity was measured in quadruplicates and expressed as percentage of that of vehicle-treated cells. Symbols represent mean values \pm SEM of 9 separate experiments.

Amantadine increased cell viability in a concentration-dependent manner, there was no effect up to 30 μ M, a significant protection at 100 μ M ($p < 0.05$ by Student's t-test) and at 300 μ M cell viability was increased to about 80 % of untreated cells.

3.5.2. NR1/2A-receptor induced cytotoxicity

In cells expressing the NR1A/2A receptor under the control of the T-RexTM system cytotoxicity was induced by treatment with tetracycline, eliciting the synthesis of NMDARs which are excitotoxic presumably due to constant Ca^{2+} influx into the cell triggering apoptosis.

Treatment of the cells with drugs blocking the NMDA receptor increased cell viability in a concentration-dependent manner. The noncompetitive antagonist at the NMDA receptor ketamine was tested in the concentration range of 3 to 1000 μM (Fig.39).

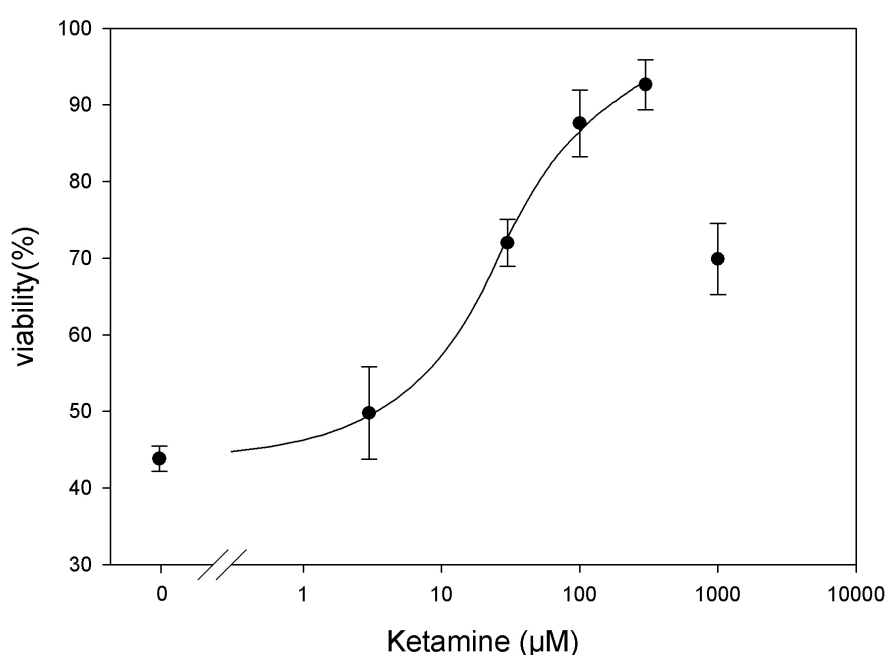


Fig. 39: Effect of ketamine on toxicity induced by NMDA receptor expression. Cells expressing the NR1/2A-receptor under the control of the T-RexTM were seeded in 96-well plates and on the next day the NR1/2A-receptor was induced by treatment with tetracycline and ketamine was added at the concentrations indicated. Cell viability was determined by measuring acid phosphatase activity 24 hrs after treatment. Activity was measured in quadruplicates and expressed as percentage of the activity in uninduced cells. Symbols represent mean values \pm SEM of 3 separate experiments.

Ketamine increased cell viability in a concentration-dependent manner at concentrations up to 300 μM which restored viability to more than 90 % of uninduced cells. At 1000 μM a marked reduction in viability to 70 % was observed.

In another series of experiments I tested the noncompetitive antagonist memantine in the concentration-range of 1 to 300 μM (Fig.40).

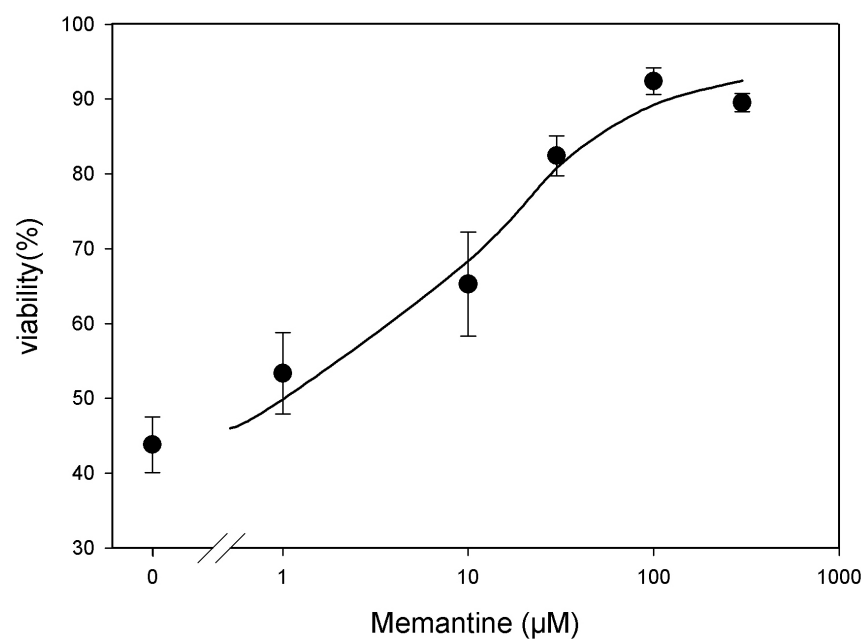


Fig. 40: Effect of memantine on toxicity induced by NMDA receptor expression. Cells expressing the NR1/2A-receptor under the control of the T-RexTM were seeded in 96-well plates and one day later the NR1/2A-receptor was induced by treatment with tetracycline and memantine was added at the concentrations indicated. Cell viability was determined by measuring acid phosphatase activity 24 hrs after treatment. Activity was measured in quadruplicates and expressed as percentage of that of uninduced cells. Symbols represent mean values \pm SEM of 3 separate experiments.

Memantine increased cell viability concentration dependently reaching a maximum protective effect at 100 μ M with a viability of about 90 % of uninduced cells.

Finally, I tested amantadine for its protective action against NMDA-receptor induced cytotoxicity in the concentration range of 1 to 300 μ M (Fig. 41).

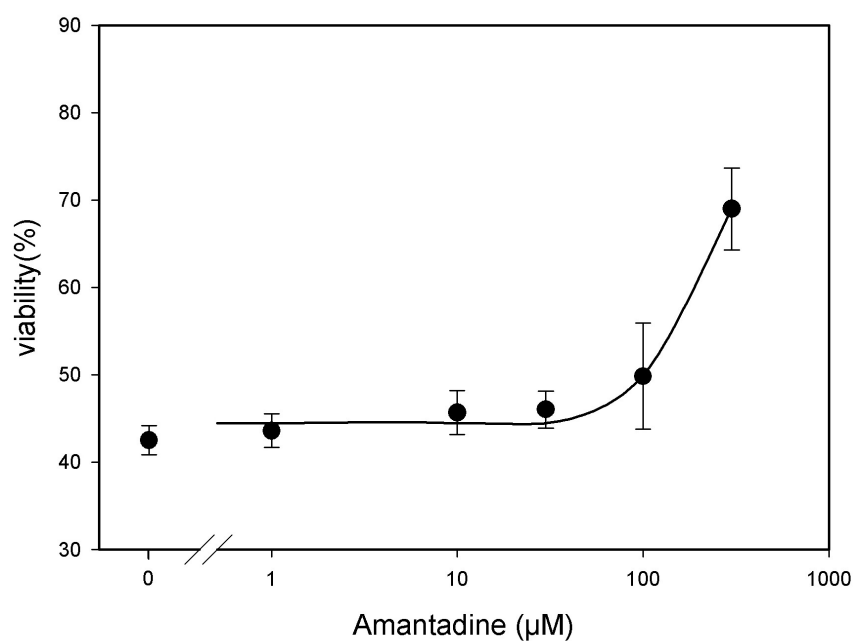


Fig. 41: Effect of amantadine on toxicity induced by NMDA receptor expression. Cells expressing the NR1/2A-receptor under the control of the T-RexTM were seeded in 96-well plates and one day later the NR1/2A-receptor was induced by treatment with tetracycline and amantadine was added at the concentrations indicated. Cell viability was determined by measuring acid phosphatase activity 24 hrs later. Activity was measured in quadruplicates and expressed as percentage of that of uninduced cells. Symbols represent mean values \pm SEM of 4 separate experiments.

Amantadine had no significant effect in concentrations up to 100 μ M. At 300 μ M amantadine significantly antagonized the NMDA-receptor induced cytotoxicity ($p < 0.05$ by Student's t-test), but only restored cell viability to about 70 % of uninduced cells.

4. Discussion

Back in the 1960s amantadine was only used for the prophylaxis and treatment of influenza A acting as an inhibitor of a viral integral membrane protein necessary for uncoating. Later on in the 1970s observations showed that amantadine was beneficial for the treatment of PD, as it could substantially reduce Parkinsonian symptoms. Today amantadine is a standard first line therapy in PD and is administered together with levodopa and DA receptor agonists—and muscarinreceptor antagonists. Besides of its weak NMDAR blocking properties amantadine has been shown in several studies to increase extracellular DA and NA levels.

Since plasmalemmal monoamine transporters are decisively involved in the regulation of extracellular NA and DA concentrations, the scope of my work was to compare the action of amantadine on NAT and DAT with its action on the NMDA receptor. Furthermore, for the first time the interaction of amantadine with the human variants of these proteins should be studied. Finally, the interaction should be investigated on living cells in order to reproduce *in vivo* conditions for the human proteins. In contrast to radioligand binding assays, which would be another option to study the molecular pharmacology of a drug, assays on living cells have the advantage that transporters or receptors are embedded in their natural environment in terms of ion distribution and membrane potential.

For investigation of the role of amantadine as a possible releaser of NA and DA I used HEK293 cells which heterologously expressed the human NAT or DAT. In uptake experiments amantadine was able to block the transport of radiolabelled substrates into both types of cells. However, amantadine was 15 times more potent in inhibiting uptake by the NAT than by the DAT. Also in previous work on rat brain preparations amantadine was more potently inhibiting uptake into NA than into DA rich regions (Herblin 1971; Baldessarini et al. 1972; Thornburg and Moore, 1973). The next question was if amantadine was a pure uptake inhibitor or a releasing drug, because both, uptake blockers and releasing drugs, behave similar in uptake experiments. Therefore, I did superfusion experiments by which I was able to distinguish between both types of drugs. In superfusion experiments on NAT expressing cells, amantadine clearly demonstrated a releasing action however the maximum effect was less than half of that of amphetamine. The pure uptake inhibitor mazindol was able to block the releasing action of both, amphetamine and amantadine. This finally confirmed that amantadine is a releaser like amphetamine.

Recent studies on amphetamine research show that reverse transport is dependent on intracellular phosphorylation of the N-terminus of DAT (Khoshbouei, Sen et al. 2004). Amphetamine-induced reverse transport is also abolished in NAT if there is no phosphorylation of the N-terminus (Kantor, Hewlett et al. 2001). Amphetamine induced activation of PKC and CaMKII seems to be crucial for the phosphorylation of the N-terminus which leads to the association of syntaxin1A. All these factors together promote the shift of DAT from a reluctant state to a willing state for amphetamine-induced DA-efflux (Robertson, Matthies et al. 2009). With special inhibitors of PKC and CaMKII (staurosporine) or Syntaxin 1 A in DAT and NAT expressing cells with subsequent superfusion with amantadine and amphetamine as control it could be clarified in future experiments if amantadine acts through the same intracellular mechanisms as amphetamine.

Patch-clamp experiments are another approach to elucidate the type of drug interaction with a transporter. The translocation process in the DAT or NAT is an electrogenic process because the cotransport of sodium ions results in the influx of one or two positive charges for each molecule of DA or NA pumped into the cell. Additional ion fluxes might be due to a channel-like mode of the transporters triggered by the interaction with substrates as suggested in several reports. Releasing drugs behave like transporter substrates and induce inward currents in voltage-clamp experiments in the whole-cell configuration. Therefore, my patch-clamp experiments also revealed that amantadine was a releasing drug at the NAT. Ten and 30 μM amantadine induced inward currents. These currents were smaller than that induced by amphetamine. This is in agreement with the weak releasing action of amantadine in superfusion experiments. The question, if the maximum inward current to be elicited by amantadine is also smaller than that elicited by amphetamine, would require data on higher concentrations of amantadine in patch-clamp experiments. However, the finding that the NA-induced inward current was smaller in the presence of amantadine suggests that amantadine is in fact a kind of “partial releaser”, following the concept of partial agonism in receptor pharmacology, where drugs are called partial agonists if they stimulate signal transduction at receptors, but to a smaller extent than full agonists.

The superfusion of 10 μM amantadine on DAT cells produced no significant inward currents and the application of 10 μM NA in the presence of 30 μM amantadine led to a negligible attenuation of the NA evoked inward current ($p>0.05$) at the DAT. These findings suggest that

amantadine has a lower affinity at the DAT than at the NAT and are in agreement with the uptake data.

To study the interaction of amantadine with a human NMDA receptor I established cell lines stably expressing a receptor consisting of the two subunits NR1 and NR2A, which are most widely distributed in the brain (Mori and Mishina, 1995), under the control of the T-RexTM system. Although binding of the radioligand MK801 by the various clones was rather weak compared to brain tissue, the NMDA receptor was functionally active as revealed by the strong toxicity if the receptor was induced in cells. The well-known noncompetitive NMDA-receptor antagonist ketamine efficiently blocked cytotoxicity in the μ molar range restoring cell viability to more than 90 % of that of cells without NMDA-receptor induction. By contrast, amantadine was not protective at 100 μ M and only partly at 300 μ M.

In the cytotoxicity paradigm actions of the drugs in a time scale of more than 24 hrs are relevant. In order to study long-term blocking effects on the NAT as well, I investigated the interference of amantadine with the cytotoxic effect of MPP⁺ on NAT expressing cells. In this model the highly NAT-selective tricyclic antidepressant drug desipramine had the highest potency and efficacy in blocking the MPP⁺-induced toxicity. Amantadine was much less potent than desipramine, but 100 μ M had a significant, and 300 μ M a strong protective effect, restoring cell viability to 80 % of vehicle treated cells. It is interesting to note that in the superfusion experiment there was no difference between the releasing effect of 100 μ M and 300 μ M amantadine whereas in the toxicity assay 300 μ M amantadine were clearly more effective. The mechanism of cytoprotection is the blockade of the MPP⁺ transport into the cell, whereas for induction of release amantadine acts as substrate and induces reverse transport.

In conclusion, based on my results, amantadine is at least as potently inhibiting the human NAT as blocking the human NMDA receptor. Although my experiments on transfected cells obviously could not definitely establish amantadine's mode of action in PD, the molecular pharmacology as demonstrated in my work is not incompatible with a noradrenergic mechanism.

5. References

- Amara, S. G. (1992). "Neurotransmitter transporters. A tale of two families." Nature **360**(6403): 420-1.
- Aoki, F. Y. and D. S. Sitar (1985). "Amantadine kinetics in healthy elderly men: implications for influenza prevention." Clin Pharmacol Ther **37**(2): 137-44.
- Arai, A., K. Kannari, et al. (2003). "Amantadine increases L-DOPA-derived extracellular dopamine in the striatum of 6-hydroxydopamine-lesioned rats." Brain Res **972**(1-2): 229-34.
- Baldessarini, R.J., J.F. Lipinski, et al. (1972). "Effects of amantadine hydrochloride on catecholamine metabolism in the brain of the rat." Biochem Pharmacol. **21**(1):77-87.
- Basler, C. F. (2007). "Influenza viruses: basic biology and potential drug targets." Infect Disord Drug Targets **7**(4): 282-93.
- Bear, M. F., B.W. Connors, M.A Paradiso (2001). Neurotransmitter systems. Neuroscience: exploring the brain. S. Katz. Baltimore, Lippincot Williams and Wilkins: 855.
- Bezard, E., C. Brefel, et al. (1999). "Effect of the alpha 2 adrenoreceptor antagonist, idazoxan, on motor disabilities in MPTP-treated monkey." Prog Neuropsychopharmacol Biol Psychiatry **23**(7): 1237-46.
- Blanchet, P.J., S. Konitsiotis, et al. (1998). "Amantadine reduces levodopa-induced dyskinesias in parkinsonian monkeys." Mov Disord. **13**(5):798-802
- Blanpied, T. A., R. J. Clarke, et al. (2005). "Amantadine inhibits NMDA receptors by accelerating channel closure during channel block." J Neurosci **25**(13): 3312-22.
- Boman, K. and J. Porras (1970). "Amantadine treatment of Parkinson's disease." Acta Neurol Scand **46**: Suppl 43:225+.
- Bonisch, H. (1998). "Transport and drug binding kinetics in membrane vesicle preparation." Methods Enzymol **296**: 259-78.
- Bonisch, H. and M. Bruss (2006). "The norepinephrine transporter in physiology and disease." Handb Exp Pharmacol(175): 485-524.
- Bonisch, H., R. Hammermann, et al. (1998). "Role of protein kinase C and second messengers in regulation of the norepinephrine transporter." Adv Pharmacol **42**: 183-6.
- Bordet, R., S. Ridray, et al. (1997). "Induction of dopamine D3 receptor expression as a mechanism of behavioral sensitization to levodopa." Proc Natl Acad Sci U S A **94**(7): 3363-7.
- Buck, K. J. and S. G. Amara (1994). "Chimeric dopamine-norepinephrine transporters delineate structural domains influencing selectivity for catecholamines and 1-methyl-4-phenylpyridinium." Proc Natl Acad Sci U S A **91**(26): 12584-8.

- Calon, F. and T. Di Paolo (2002). "Levodopa response motor complications--GABA receptors and preproenkephalin expression in human brain." Parkinsonism Relat Disord **8**(6): 449-54.
- Calon, F., A. H. Rajput, et al. (2003). "Levodopa-induced motor complications are associated with alterations of glutamate receptors in Parkinson's disease." Neurobiol Dis **14**(3): 404-16.
- Cull-Candy, S., S. Brickley, et al. (2001). "NMDA receptor subunits: diversity, development and disease." Curr Opin Neurobiol **11**(3): 327-35.
- Eymin, C., Y. Charnay, et al. (1995). "Localization of noradrenaline transporter mRNA expression in the human locus coeruleus." Neurosci Lett **193**(1): 41-4.
- Farnebo, L. O., K. Fuxe, et al. (1971). "Dopamine and noradrenaline releasing action of amantadine in the central and peripheral nervous system: a possible mode of action in Parkinson's disease." Eur J Pharmacol **16**(1): 27-38.
- Fletcher, E.A., P.H. Redfern (1970). " The effect of amantadine on the uptake of dopamine and noradrenaline by rat brain homogenates." J Pharm Pharmacol. **22**(12):957-9.
- Friedrich, U. and H. Bonisch (1986). "The neuronal noradrenaline transport system of PC-12 cells: kinetic analysis of the interaction between noradrenaline, Na⁺ and Cl⁻ in transport." Naunyn Schmiedebergs Arch Pharmacol **333**(3): 246-52.
- Gainetdinov, R. R., T. D. Sotnikova, et al. (2002). "Monoamine transporter pharmacology and mutant mice." Trends Pharmacol Sci **23**(8): 367-73.
- Galli, A., L.J. DeFelice, et al. (1995). "Sodium-dependent norepinephrine-induced currents in norepinephrine-transporter-transfected HEK-293 cells blocked by cocaine and antidepressants." J Exp Biol. **198**(Pt 10):2197-212
- Gesi, M., P. Soldani, et al. (2000). "The role of the locus coeruleus in the development of Parkinson's disease." Neurosci Biobehav Rev **24**(6): 655-68.
- Grelak, R. P., R. Clark, et al. (1970). "Amantadine-dopamine interaction: possible mode of action in Parkinsonism." Science **169**(941): 203-4.
- Herblin, W.F. (1972). "Amantadine and catecholamine uptake." Biochem Pharmacol. **21**(14):1993-5.
- Iversen, L. L. (1971). "Role of transmitter uptake mechanisms in synaptic neurotransmission." Br J Pharmacol **41**(4): 571-91.
- Kantor, L., G. H. Hewlett, et al. (2001). "Protein kinase C and intracellular calcium are required for amphetamine-mediated dopamine release via the norepinephrine transporter in undifferentiated PC12 cells." J Pharmacol Exp Ther **297**(3): 1016-24.
- Karp, S.J., M. Masu, et al. (1993). " Molecular cloning and chromosomal localization of the key subunit of the human N-methyl-D-aspartate receptor." J Biol Chem. **268**(5):3728-33.
- Kasper, S., Giamal N. el, et al., (2000). "Reboxetine: the first selective noradrenaline re-uptake inhibitor." Expert Opin.Pharmacother. **1**(4):771-782.

- Khoshbouei, H., H. Wang, et al. (2003). "Amphetamine-induced dopamine efflux. A voltage-sensitive and intracellular Na⁺-dependent mechanism." J Biol Chem. **278**(14):12070-7.
- Khoshbouei, H., N. Sen, et al. (2004). "N-terminal phosphorylation of the dopamine transporter is required for amphetamine-induced efflux." PLoS Biol **2**(3): E78.
- Kornhuber, J., J. Bormann, et al. (1991). "Effects of the 1-amino-adamantanes at the MK-801-binding site of the NMDA-receptor-gated ion channel: a human postmortem brain study." Eur.J Pharmacol. **206** (4):297-300.
- Langer, S.Z. (1980). "Presynaptic regulation of the release of catecholamines." Pharmacol Rev. **32**(4):337-62.
- Lategan, A. J., M. R. Marien, et al. (1992). "Suppression of nigrostriatal and mesolimbic dopamine release in vivo following noradrenaline depletion by DSP-4: a microdialysis study." Life Sci **50**(14): 995-9.
- Lim, E. (2005). "A walk through the management of Parkinson s disease." Ann Acad Med Singapore **34**(2): 188-95.
- Liu, Y. and J. Zhang (2000). "Recent development in NMDA receptors." Chin Med J (Engl) **113**(10): 948-56.
- Loland, C.J., L. Norregaard, et al. (2002). "Generation of an activating Zn(2+) switch in the dopamine transporter: mutation of an intracellular tyrosine constitutively alters the conformational equilibrium of the transport cycle." Proc Natl Acad Sci U S A. **99**(3):1683-8.
- Lu, D., K. Yu, et al. (1996). "Regulation of norepinephrine transport system by angiotensin II in neuronal cultures of normotensive and spontaneously hypertensive rat brains." Endocrinology **137**(2): 763-72.
- Lusis, S. A. (1997). "Pathophysiology and management of idiopathic Parkinson's disease." J Neurosci Nurs **29**(1): 24-31.
- Mandela, P. and G. A. Ordway (2006). "The norepinephrine transporter and its regulation." J Neurochem **97**(2): 310-33.
- Marshall, J. F. and U. Ungerstedt (1977). "Supersensitivity to apomorphine following destruction of the ascending dopamine neurons: quantification using the rotational model." Eur J Pharmacol **41**(4): 361-7.
- McAuley, J. H. (2003). "The physiological basis of clinical deficits in Parkinson's disease." Prog Neurobiol **69**(1): 27-48.
- McElvain, J. S. and J. O. Schenk (1992). "A multisubstrate mechanism of striatal dopamine uptake and its inhibition by cocaine." Biochem Pharmacol **43**(10): 2189-99.
- Melikian, H. E., S. Ramamoorthy, et al. (1996). "Inability to N-glycosylate the human norepinephrine transporter reduces protein stability, surface trafficking, and transport activity but not ligand recognition." Mol Pharmacol **50**(2): 266-76.

- Mori, H. and M. Mishina (1995). "Structure and function of the NMDA receptor channel." Neuropharmacology **34**(10):1219-1237.
- E. Neher and B. Sakmann (1976). "Single-channel currents recorded from membrane of denervated frog muscle fibres". Nature **260** (5554):799-802.
- Nelson, N. (1998). "The family of Na⁺/Cl⁻ neurotransmitter transporters." J Neurochem **71**(5): 1785-803.
- Olivier, B., W. Soudijn, et al. (2000). "Serotonin, dopamine and norepinephrine transporters in the central nervous system and their inhibitors." Prog Drug Res **54**: 59-119.
- Pacholczyk, T., R. D. Blakely, et al. (1991). "Expression cloning of a cocaine- and antidepressant-sensitive human noradrenaline transporter." Nature **350**(6316): 350-4.
- Papa, S. M., R. Desimone, et al. (1999). "Internal globus pallidus discharge is nearly suppressed during levodopa-induced dyskinesias." Ann Neurol **46**(5): 732-8.
- Peyro Saint Paul, H., O. Rascol, et al. (1995). "Short term oral administration of idazoxan in mild stable parkinsonian patients treated with L-Dopa." First Congress of the European Association for Clinical Pharmacology and Therapeutics. 27-30: Paris, 172
- Piffl, C., E. Agneter, et al. (1997). "Induction by low Na⁺ or Cl⁻ of cocaine sensitive carrier-mediated efflux of amines from cells transfected with the cloned human catecholamine transporters." Br J Pharmacol **121**(2): 205-12.
- Piffl, C., O. Hornykiewicz, et al. (1996). "Catecholamine transporters and 1-methyl-4-phenyl-1,2,3,6-tetrahydropyridine neurotoxicity: studies comparing the cloned human noradrenaline and human dopamine transporter." J.Pharmacol.Exp.Ther. **277**(3):1437-1443.
- Rascol, O., I. Arnulf, et al. (2001). "Idazoxan, an alpha-2 antagonist, and L-DOPA-induced dyskinesias in patients with Parkinson's disease." Mov Disord. **16**(4):708-13.
- Ravna, A. W., I. Sylte, et al. (2003). "Molecular model of the neural dopamine transporter." J Comput Aided Mol Des **17**(5-6): 367-82.
- Rinne, U. K. (1982). "Parkinson's disease as a model for changes in dopamine receptor dynamics with aging." Gerontology **28 Suppl 1**:35-52. Review.
- Robertson, S. D., H. J. Matthies, et al. (2009). "A closer look at amphetamine-induced reverse transport and trafficking of the dopamine and norepinephrine transporters." Mol Neurobiol **39**(2): 73-80.
- Rommelfanger, K. S. and D. Weinshenker (2007). "Norepinephrine: The redheaded stepchild of Parkinson's disease." Biochem Pharmacol **74**(2): 177-90.
- Scatton, B., A. Cheramy, et al. (1970). "Increased synthesis and release of dopamine in the striatum of the rat after amantadine treatment." Eur J Pharmacol. **13**(1):131-3.

- Schmidt, W.J.(1995). "Balance of transmitter activities in the basal ganglia loops." J Neural Transm Suppl. **46**: 67-76. Review.
- Schroeter, S., S. Apparsundaram, et al. (2000). "Immunolocalization of the cocaine- and antidepressant-sensitive l-norepinephrine transporter." J Comp Neurol **420**(2): 211-32.
- Sharp, S. I., A. McQuillin, et al. (2009). "Genetics of attention-deficit hyperactivity disorder (ADHD)." Neuropharmacology **57**(7-8): 590-600.
- H. H. Sitte, H. H., S. Huck, et al. (1998) "Carrier-mediated release, transport rates, and charge transfer induced by amphetamine, tyramine, and dopamine in mammalian cells transfected with the human dopamine transporter." J.Neurochem. **71** (3):1289-1297.
- Smith, H.R., T.J. Beveridge, et al. (2006). "Distribution of norepinephrine transporters in the non-human primate brain." Neuroscience. **138**(2):703-14.
- Spilker, B.A., K.M. Dhasmana (1974). "On the specificity of dopamine release by amantadine." Experientia. **30**: 64-65
- Stoof, J.C., J. Booij (1992). " Amantadine as N-methyl-D-aspartic acid receptor antagonist: new possibilities for therapeutic applications?" Clin Neurol Neurosurg. **94** Suppl:S4-6.
- Sulzer, D., M. S. Sonders, et al. (2005). "Mechanisms of neurotransmitter release by amphetamines: a review." Prog Neurobiol **75**(6): 406-33.
- Syringas, M., F. Janin, et al. (2000). "Structural domains of chimeric dopamine-noradrenaline human transporters involved in the Na(+)- and Cl(-)-dependence of dopamine transport." Mol Pharmacol **58**(6): 1404-11.
- Takahashi, T., H. Yamashita, et al. (1996). "Inhibitory effect of MK-801 on amantadine-induced dopamine release in the rat striatum." Brain Res Bull **41**(6): 363-7.
- Thornburg, J.E., Moore, K.E (1973). " Dopamine and norepinephrine uptake by rat brain synaptosomes: relative inhibitory potencies of l- and d-amphetamine and amantadine." Res Commun Chem Pathol Pharmacol. **5**(1):81-9.
- Trendelenburg, U. (1991). "The TiPS lecture: functional aspects of the neuronal uptake of noradrenaline." Trends Pharmacol Sci **12**(9): 334-7.
- Ungerstedt, U. (1971). "Striatal dopamine release after amphetamine or nerve degeneration revealed by rotational behaviour." Acta Physiol Scand Suppl **367**: 49-68.
- van der Zwaluw, C. S., R. C. Engels, et al. (2009). "Polymorphisms in the dopamine transporter gene (SLC6A3/DAT1) and alcohol dependence in humans: a systematic review." Pharmacogenomics **10**(5): 853-66.
- Vaughan, R. A. (1995). "Photoaffinity-labeled ligand binding domains on dopamine transporters identified by peptide mapping." Mol Pharmacol **47**(5): 956-64.

Verhagen Metman L., P. Del Dotto, et al. (1998). "Amantadine as treatment for dyskinesias and motor fluctuations in Parkinson's disease." Neurology. **50**(5):1323-6.

Vernier, V. G., J. B. Harmon, et al. (1969). "The toxicologic and pharmacologic properties of amantadine hydrochloride." Toxicol Appl Pharmacol **15**(3): 642-65.

Volz, T. J. and J. O. Schenk (2005). "A comprehensive atlas of the topography of functional groups of the dopamine transporter." Synapse **58**(2): 72-94.

Yang, T.T., P. Sinai, et al. (1996). "An acid phosphatase assay for quantifying the growth of adherent and nonadherent cells." Anal Biochem. **241**(1):103-8

Zahniser, N. R. and S. Doolen (2001). "Chronic and acute regulation of Na⁺/Cl⁻-dependent neurotransmitter transporters: drugs, substrates, presynaptic receptors, and signaling systems." Pharmacol Ther **92**(1): 21-55.

Zhou, Z., J. Zhen, et al. (2007). "LeuT-desipramine structure reveals how antidepressants block neurotransmitter reuptake." Science **317**(5843): 1390-3.

Curriculum Vitae

Christian Sommerauer

1180 Wien
Erndtgasse42/7
06504539645
a0040149@unet.univie.ac.at

Geburtsdatum	18 November 1980
Geburtsort	Wien
Staatsbürgerschaft	Österreich
Religion	o.B.

Ausbildung

Volksschule 1987-1991	1180 Wien, Bischof Faber Platz
--------------------------	--------------------------------

Gymnasium 1991-1999 06/1999	1180 Wien, Haizingergasse Matura
-----------------------------------	-------------------------------------

Zivildienst 1999-2000	1150 Wien, Arbeiter-Samariter-Bund
--------------------------	------------------------------------

10/2000-03/2010	Magisterstudium der Molekularen Biologie (Universität Wien) Schwerpunkte: Immunologie, Neurobiologie, Bioinformatik Diplomarbeit: "Molecular pharmacology of amantadine and related drugs in cells heterologously expressing human transporters and receptors"
-----------------	---

Sprachkenntnisse

Englisch, Französisch

Ferialjobs und Praktika

2004	St.Martin Apotheke
------	--------------------